

PRODUCTION OF SUSTAINABLE BUTANOL BIOFUEL FROM CORN STOVER

A Technical Report

In CHE 4476

Presented to

The Faculty of the

School of Engineering and Applied Science

University of Virginia

In Partial Fulfillment of the Requirements for the Degree

Bachelor of Science in Chemical Engineering

By

Kevin London, Isabella Powell, Rachel Rosner,

Jason Thielen, & Olivia Wilkinson

May 10th, 2024

On my honor as a University student, I have neither given nor received unauthorized aid on this assignment as defined by the Honor Guidelines for Thesis-Related Assignments.

ADVISOR

Eric Anderson, Department of Chemical Engineering

Table of Contents

1. Table of Contents	2
2. Figures, Tables, and Equations Table of Contents	6
3. Executive Summary	10
4. Introduction	11
5. Previous Work	13
6. Discussion	15
6.1 Storage	16
6.1.1 <i>Feedstock Storage</i>	16
6.1.2 <i>Product Storage</i>	17
6.2 Milling	19
6.3 Acid Pretreatment	19
6.3.1 <i>Dilute Phosphoric Acid Hydrolysis of Corn Stover</i>	19
6.3.2 <i>Neutralization of Phosphoric acid with Calcium Hydroxide</i>	24
6.3.3 <i>Filter Design</i>	27
6.4 Fermentation	29
6.4.1 <i>Main Reactor Kinetics</i>	29
6.4.2 <i>Main Fermentation Reactor Design</i>	33
6.4.3 <i>Seed Reactor Design</i>	33
6.5 Separations	35
6.5.1 <i>Hydrophobic Pervaporation</i>	36
6.5.2 <i>Decanter and Recycle Design</i>	38
6.5.2.1 <i>Phase Separation</i>	38

6.5.2.2 Decanter Design.....	39
6.5.2.3 Recycle Column.....	40
6.5.3 Hydrophilic Pervaporation.....	42
6.5.4 ABE Column.....	43
6.5.5 O’Connell Correlation.....	46
<u>6.6 Auxiliary Equipment.....</u>	48
6.6.1 Heat Exchangers.....	48
6.6.2 Pumps.....	49
6.6.3 Conveyors.....	51
6.6.4 Compressors.....	52
<u>7. Economics.....</u>	54
7.1 Detailed Equipment Costing.....	54
7.2 Total Plant Capital Cost.....	66
7.3 Feed Costs and Product Revenue.....	67
7.4 Total Operating Costs.....	69
7.5 Cash Flow and DCF Analysis.....	71
7.5.1 Cash Flow Calculation.....	71
7.5.2 DCF Analysis and IRR Calculation.....	73
<u>8. Safety, Health, Environment, and Social.....</u>	75
8.1 Introduction.....	75
8.2 Chemical Hazard Table.....	75
8.3 Chemical Reactivity Matrix.....	76
8.4 Storage Safety Analysis.....	77

8.5 Milling Safety Analysis.....	80
8.6 Acid Pretreatment Safety Analysis.....	81
8.7 Fermentation Safety Analysis.....	82
8.8 Separations Safety Analysis.....	82
8.9 Safety Conclusion.....	88
8.10 Environment.....	88
8.11 Social.....	90
8.12 Safety Appendix.....	92
<u>9. Final Recommended Design</u>	94
9.1 Nomenclature.....	94
9.2 Storage (Block A).....	96
9.2.1 Feedstock Storage.....	96
9.2.2 Product Storage.....	96
9.3 Milling (Block B).....	97
9.4 Acid Pretreatment (Block C).....	99
9.5 Fermentation (Block D).....	103
9.5.1 Seed Fermentation.....	104
9.5.2 Primary Fermentation.....	104
9.6 Separations Block (Block E).....	106
<u>10. Conclusions and Recommendations</u>	109
<u>10.1 Future Research Suggestions</u>	109
10.1.1 CaHPO ₄ Animal Feed.....	109
10.1.2 Clostridium.....	110

10.1.3 <i>Simulation Environments</i>	110
<u>10.2 <i>Design Improvements</i></u>	111
10.2.1 <i>Evaluating Solids Removal</i>	111
10.2.2 <i>Optimizing Fermentation Parameters</i>	111
10.2.3 <i>Separations: Decantation</i>	112
10.2.4 <i>Pumps</i>	112
10.2.5 <i>Pervaporation</i>	112
10.2.6 <i>Waste Disposal</i>	113
<u>10.3 <i>Future Extensions of the Project / Continued Work</i></u>	113
<u>10.4 <i>Final Recommendations</i></u>	114
<u>11. Acknowledgements</u>	115
<u>12. References</u>	116

2. Figures, Tables, and Equations Table of Contents

<i>Figure 6 Simplified BFD</i>	16
<u>Discussion: Acid Pretreatment (Section 6.3)</u>	20
<i>Figure 6.3.1a Reactor Layout for Dilute Acid Hydrolysis</i>	22
<i>Figure 6.3.1b Hydrolysis Reactor Schedule</i>	23
<i>Table 6.3.1a Compositions and Flow Rates for Dilute Acid Hydrolysis</i>	24
<i>Equation 6.3.2a Neutralization Reaction</i>	25
<i>Table 6.3.2a Neutralization Electrolyte Wizard Inputs and Reactions</i>	26
<i>Table 6.3.2b Compositions and Flow Rates for Neutralization before Filtration</i>	27
<i>Figure 6.3.2a Neutralization Process Flow Diagram</i>	28
<i>Figure 6.3.3a Calculation for Disk Filter Area</i>	29
<u>Discussion: Fermentation (Section 6.4)</u>	30
<i>Table 6.4.1a Ordinary Differential Equations for Fermentation Model</i>	31
<i>Table 6.4.1b Fermenter Conditions</i>	32
<i>Figure 6.4.3a Seed Train Schematic</i>	35
<u>Discussion: Separations (Section 6.5)</u>	36
<i>Figure 6.5a Simplified process flow diagram of separations block</i>	36
<i>Table 6.5.1a Flux Values by Material for POMS Membrane</i>	38
<i>Figure 6.5.1a PFD and Stream Composition of Hydrophobic Pervaporation</i>	38
<i>Figure 6.5.2.1a Ternary Phase Diagram</i>	40
<i>Figure 6.5.2.2a Example Design of Gravity Decanter</i>	41
<i>Figure 6.5.2.3a Decanter Recycle Column PFD</i>	42
<i>Table 6.5.2a Recycle Column Sizing and Energy Specifications</i>	43

<i>Table 6.5.3a Flux Values for Material across PDMS/Ceramic Composite Membrane</i>	44
<i>Figure 6.5.3a PFD with Stream Material Composition of Hydrophilic Pervaporation</i> ...	44
<i>Figure 6.5.4a ABE Distillation Column PFD</i>	45
<i>Figure 6.5.4b ABE & Water Vapor Pressure versus Temperature</i>	46
<i>Table 6.5.4a ABE Column Sizing and Energy Specifications</i>	47
<i>Equation 6.5.5a The O'Connell Correlation</i>	47
<u>Discussion: Auxiliary Equipment (Section 6.6)</u>	48
<i>Equation 6.6.1a Heat Exchanger Equation</i>	48
<i>Equation 6.6.1b The Total Heat Transfer Requirement Equation</i>	49
<i>Equation 6.6.2a Pump Power Equation</i>	50
<i>Table 6.6.3a Preliminary conveyor belt details</i>	52
<u>Economics (Section 7)</u>	54
<i>Equation 7.1a Pump Energy Cost Equation</i>	54
<i>Table 7.1a Conveyor Capital and Operating Cost Information</i>	57
<i>Table 7.1b Pump Capital and Operating Cost Information</i>	57
<i>Table 7.1c Tank Capital Cost Information</i>	60
<i>Table 7.1d Heat Exchanger Capital and Operating Cost Information</i>	61
<i>Table 7.1e Reactor Capital Cost Information</i>	62
<i>Table 7.1f Distillation Column Capital and Operating Cost Information</i>	63
<i>Table 7.1g Other Separations Process Capital Cost Information</i>	64
<i>Table 7.1h Compressor Capital and Operating Cost Information</i>	64
<i>Table 7.1i Hammer Mill Capital and Operating Cost Information</i>	65
<i>Table 7.2a. Capital cost broken down by equipment type</i>	66

<i>Equation 7.2a. Conversion from old price data to new price data using CEPCI.....</i>	<i>67</i>
<i>Table 7.3a Yearly Cash Flow: Feedstock & Product Cost and Revenue.....</i>	<i>68</i>
<i>Table 7.4a Total Operating Costs with reduction from ethanol and acetone burning.....</i>	<i>69</i>
<i>Table 7.4b Nonmaterial Operating Costs.....</i>	<i>70</i>
<i>Equation 7.5.1a Depreciation equation.....</i>	<i>71</i>
<i>Figure 7.5.1a. The before and after tax cash flows from year -2 to year 20.....</i>	<i>72</i>
<i>Figure 7.5.1b. The cumulative cash flow over 20 years.....</i>	<i>73</i>
<i>Equation 7.4.2a Discounted Cash Flow Equation.....</i>	<i>73</i>
<u>Safety, Health, Environment, and Social (Section 8)</u>	<i>75</i>
<i>Table 8.2a Chemical Hazards.....</i>	<i>76</i>
<i>Figure 8.3a Chemical Reactivity Matrix.....</i>	<i>77</i>
<i>Figure 8.4a Storage Toxic Cloud.....</i>	<i>78</i>
<i>Figure 8.4b Storage Pool Fire.....</i>	<i>79</i>
<i>Figure 8.4c Storage Tank BLEVE.....</i>	<i>80</i>
<i>Figure 8.8a Toxic Cloud from Acetone & Ethanol Product Stream.....</i>	<i>84</i>
<i>Figure 8.8b Flammable Cloud from Acetone & Ethanol Product Stream.....</i>	<i>85</i>
<i>Figure 8.8c Overpressure map from Acetone & Ethanol Product Stream VCE.....</i>	<i>85</i>
<i>Figure 8.8d Toxic Cloud from Butanol Product Stream.....</i>	<i>86</i>
<i>Figure 8.8e Flammable Cloud from Butanol Product Stream.....</i>	<i>87</i>
<i>Figure 8.8f Overpressure map from Butanol Product Stream VCE.....</i>	<i>87</i>
<i>Safety Appendix.....</i>	<i>92</i>
<i>8.12.1 Other Chemical reactivity matrices.....</i>	<i>92</i>
<i>8.12.2 Safety Data Sheet Sources.....</i>	<i>92</i>

8.12.3 ALOHA Assumptions.....	93
Final Recommended Design (Section 9)	94
<i>Table 9.a Block Abbreviations</i>	94
<i>Table 9.b Equipment Abbreviations</i>	94
<i>Table 9.2a Streams for Block A - Storage</i>	96
<i>Figure 9.3a Milling Final Design</i>	97
<i>Table 9.3a Streams for Block B - Milling</i>	98
<i>Figure 9.4a Acid Pretreatment Final Design</i>	99
<i>Table 9.4a Streams for Block C - Acid Pretreatment</i>	100
<i>Figure 9.4b Hydrolysis Reactor Scheduling (Same as Figure 6.3.1b)</i>	101
<i>Figure 9.5a Fermentation Final Design</i>	103
<i>Table 9.5a Streams for Block D - Fermentation</i>	104
<i>Figure 9.6a Separations Final Design</i>	106
<i>Table 9.6a Streams for Block E - Separations</i>	107

3. Executive Summary

The purpose of this document is to provide a technical design with accompanying safety and economic analyses of a biobutanol plant capable of producing 57 million kilograms of butanol each year from corn stover waste. Butanol produced at this plant will be blended into gasoline to reduce reliance on fossil fuels while improving upon the shortcomings of current gasoline additives. Corn stover, a second generation feedstock, helps improve the sustainability of the project by using a waste stream while reducing problematic reliance on feedstocks that would otherwise go towards food production.

This document will outline how corn stover is broken into digestible sugars using acid hydrolysis while Acetone-Butanol-Ethanol fermentation using *Clostridium* bacteria turns these sugars into the desired butanol product. The remaining corn waste will be combined with a high value side product, calcium monohydrogen phosphate, to be sold as a nutritious animal feed supplement. Acetone and ethanol will be burned to generate steam after a separation process that creates fuel-grade butanol.

The economics of this process indicate an IRR of 13.9% and a net present value of around \$1.52 billion. Several uncertainties remain surrounding the animal feed pricing, which is especially important given that it is the main revenue driver for the plant. Given that this IRR would only be acceptable for a well-established project in a reliable market, we find that investment in our facility is not desirable. The team recommends further research be done on product pricing, manufacturing techniques, and other areas within the scope of this design to determine if this investment would be more viable at a later date.

4. Introduction

Since the industrial revolution, there has been a heavy socio-economic dependence on fossil fuels like coal, oil, and gas (United Nations 2023). Combustion processes using these fuel sources represent some of the largest contributions to the production of greenhouse gas (GHG) emissions responsible for climate change (United Nations 2023). Despite growing awareness of the link between fossil fuel usage and the damage to Earth, there has been little change in this reliance; as of 2022, 79% of all energy consumed in the United States was derived from fossil fuels. Internal combustion engines (ICEs) are significant contributors to the usage of fossil fuels and the subsequent environmental impacts, as they produce roughly 25% of GHG emissions (NASA 2023).

In an effort to reduce the impact that ICEs have on climate change, there have been extensive efforts to implement biologically derived alcohol fuels, so called “biofuels.” Biofuels, whether used as a replacement for gasoline or as an additive, decrease the usage of nonrenewable fossil fuels by recycling previously emitted atmospheric carbon instead of releasing additional carbon which had been previously sequestered in the ground. While non-alcohol biofuels exist and are produced at industrial quantities, biologically derived fuel additives are almost exclusively alcohols, and see the most use in ICEs. Currently, ethanol is the alcohol commonly added to gasoline, but research shows that butanol is a promising alternative, given that it has a lower volatility, increased ignition performance, and higher energy density than ethanol (Trindade & Santos 2017).

In addition to the opportunity to exceed current ethanol performance, there is also substantial room for improvement in ethanol generation processes. Presently, ethanol biofuel is derived from the fermentation of corn cobs, which results in over 45% of U.S. corn growth going

toward ethanol production (USDA 2023). This represents a sustainability challenge; farmland and corn that would otherwise have been a food source are being redirected to the energy sector (Tenenbaum 2008). A shift from corn cobs to corn waste as a feedstock in our project would eliminate the concerns regarding this fuel versus food debate.

The goal of this capstone project was to design a bio-butanol production facility that utilizes a second generation cellulosic feedstock to improve sustainability in internal combustion engine fuels while mitigating concerns surrounding the food-versus-fuel debate by acting as a fuel additive similar to how ethanol is currently utilized. In order to generate biobutanol from the waste stream, the team intends to utilize Acetone-Butanol-Ethanol (ABE) fermentation which creates these three products in a 3:6:1 ratio by mass, respectively. The industrial ABE fermentation process was invented in 1916 for butanol synthesis, but fell out of use after expansion of the petrochemical industry in the 1950s (Moon et al. 2016). The design team is seeking to reimplement this process now in order to produce a higher value fuel additive that is derived from a biological, sustainable feedstock.

5. Previous Work

Principles from pre-petrochemical ABE fermentation processes in addition to current ethanol fermentation practices were studied in order to inform the design of the chemical process put forth in this report.

Another key resource for this design was a previous capstone project from UVA Chemical Engineering students. Our project is a continuation of and improvement upon the capstone project published in 2014 by Mohamed Abdelrahman, Natalie Amarin, Mikel Dermer, Lauren Grisso, and Nicholas Olszowy. Their project outlined a biobutanol plant that converted corn stover into butanol, which helped lay the groundwork for our design. There were, however, several shortcomings in this work that the team felt we could improve upon. The key differences between our project and their work are the following:

- a. In the acid pretreatment process, the acid and base used were changed to overcome solubility concerns with the waste stream to ensure that the high value salt makes it into the waste stream. The actual use of the waste stream was changed from fertilizer to a nutritious animal feed supplement to increase value.
- b. In the fermentation process, the fermentation method was changed from a fed-batch process to a continuous process. This took into account updated research that has been done since the publication of the 2014 capstone project that resulted in increased yield on account of lowered product inhibition.
- c. In the separation process, a new pervaporation method was used instead of azeotropic pressure swing distillation. This was done in an attempt to reduce energy consumption during the separation stage while incorporating new technology into the old capstone.

- d. There are other minor changes and improvements to this capstone made to maximize profit, especially given the lack of economic viability of the older capstone.

All of this previous work in combination with new research and literature findings, which will be discussed in greater detail in the discussion section, informed our design and helped the team reach the design goal.

6. Discussion

Iowa, Nebraska, Illinois, and Minnesota are the top corn producers in the country. These states produce 16.2%, 15%, 12.6%, and 10% of the nations' corn - and corn stover - respectively (Cook 2023). Of these states, Iowa was selected as the most probable location largely based on corn stover input economic considerations outlined later in the memorandum. Within Iowa, the team selected a location along the Northern border for its proximity to the interstate system and surplus of corn-producing counties. Specifically, stover from Winnebago and Hancock counties was used as the basis for setting the scale of the production facility.

Due to the plant's location in Northern Iowa, the supply of dry (~6.2% water content) corn stover from the neighboring counties sets the maximum possible scale of the process at 3,490,000,000 kg of corn stover used per year (Dutton 2020). A typical industrial ethanol plant today scales at about 25-48 million gallons of ethanol produced per year (Baral et al. 2016; Clifford 2023). Because the production of biobutanol is not industrially commercialized, the target scale for this project will model a smaller-scale ethanol plant at 57 million kilograms (19 million gallons) of butanol produced per year. The following discussion sections detail by process the method of attack, design considerations, assumptions made, and final proposed designs of the desired biobutanol plant. The overall block flow diagram for the entire process is shown in Figure 6.

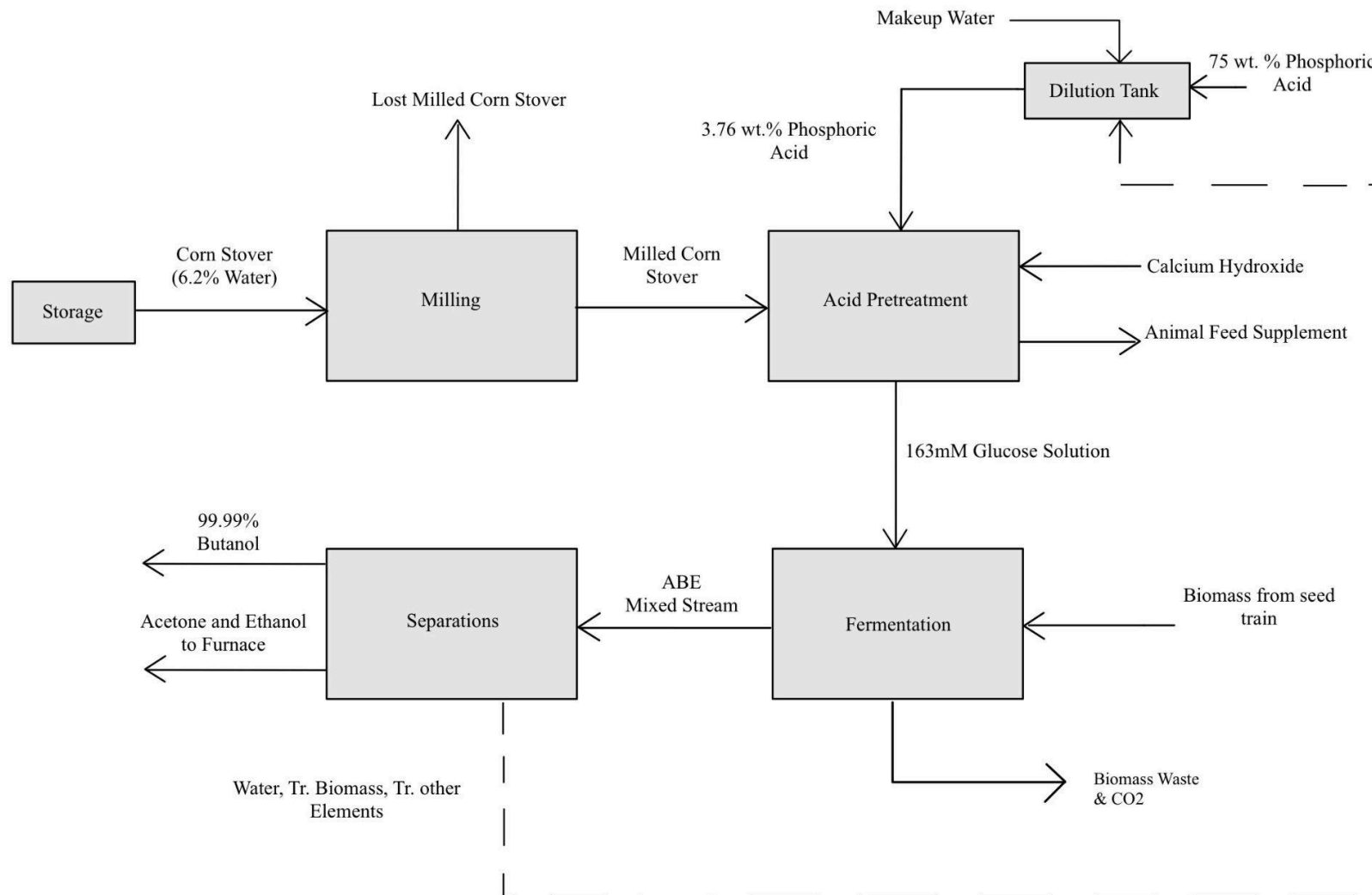


Figure 6. Simplified BFD. See Section 9 for more detailed diagrams and final process descriptions

6.1 Storage

6.1.1 Feedstock Storage

Corn in Iowa is harvested in a three month window, September through November, and therefore enough corn stover must be bought and stored to cover a year's supply of biobutanol product (*Corn FAQs*). When harvesting corn stover, one acre of corn produces about 150 bushels of corn, or about 2.1 tons of corn stover (Jiao 2016). One of the largest storage options available on an industrial level is a storage bin that can hold about 28,000,000 kg of corn stover (*Million Bushel Bins*). To accommodate a year's supply of corn stover for butanol production, 47 storage bins will be needed.

Phosphoric acid at 75 wt.% requires a corrosion resistant, double lined 316-L stainless steel vessel for proper storage (*Safety Data Sheet: Phosphoric Acid*). According to *Purified phosphoric acid*, the freezing point of phosphoric acid is highly dependent upon its ratio of acid to water. Therefore, 75 wt.% phosphoric acid can be stored outdoors without much danger of freezing, even with average Iowan winter temperatures of -8°C (*Phosphoric acid 75%; National Weather Service*). The proposed biobutanol plant requires about 0.8% of the world's total phosphoric acid production per year, resulting in almost 720,000,000 kg of 75 wt.% phosphoric acid needed. To accommodate one operating month's supply of phosphoric acid, only about 49,200,000 kg of acid are needed, necessitating the use of one floating roof tank (Peters et al. 2003). A floating roof design is used, allowing for volume fluctuation as feed is stored and transported to the plant.

One operating month's capacity of anhydrous calcium hydroxide is about 27,600,000 kg. Given (*Calcium hydroxide supply chain; Calcium hydroxide*) that this is a one month supply, the material will be used before the shelf life is reached, thus no additional inerting or other

preservation measures need to be taken(*Calcium hydroxide supply chain; Calcium hydroxide*).

One cone roof tank will be used (Peters et al. 2003) will be used to hold the material and protect it from the elements.

The bacteria, *Clostridium acetobutylicum ATCC 824*, will be utilized in the fermentation step of the biobutanol process. To save on capital costs, the plant will buy an initial batch of bacteria, and then grow subsequent cells from that initial batch. This investment will be part of a larger million dollar investment in the plant's master cell bank (see section 7.3 Feed Costs and Product Revenue). Additionally, to accommodate the need for seven seed trains in the fermentor step, several stainless steel 316-L fermentors with capacities of 500 m³, 50 m³, 5 m³, and 0.5 m³ will be needed.

6.1.2 Product Storage

To reduce capital costs associated with product storage, storage capacity was based on one operating month's worth of product for each stream.

The highest volume stream leaving the plant is a monocalcium phosphate animal feed product that will be repurposed into an animal feed supplement. The bulk of this stream will consist of digested corn stover, and therefore 21 storage bins of the same capacity and brand as the corn stover feedstock will be needed to store one month's supply of product, about 245,400,000 kg worth of material (*Million Bushel Bins*).

To save on utility costs, instead of ethanol and acetone storage, these products will be immediately burned as they are produced from the separation process. The products will be fed to a furnace to create steam that will be utilized throughout the plant.

The final butanol product will be stored in one floating roof tank (Peters et al. 2003). The floating roof tanks used in both product and feedstock storage prevent the formation of a flammable vapor space which is important for process safety.

6.2 Milling

To create a larger surface area to volume ratio better suited for hydrolysis, corn stover must be milled. A hammer mill with a 12.48mm geometric mean chop size, requiring 6.96 kWh/ton will be utilized (Mani et al. 2004). A hammer mill was found that can mill stover at 100 tons per hour (*Hammer mills: High capacity particle sizing*). According to plant requirements, 199.1 tons of stover need to be fed to the milling process, therefore 2 hammer mills will be needed to meet downstream requirements.

6.3 Acid Pretreatment

For corn stover to be turned into usable sugar for the fermentation process, an acid catalyzed hydrolysis reaction must digest cellulose into glucose. For this acidic solution to pass on to the fermentation processes without negatively impacting cellular viability, a base must be used to neutralize the solution to the optimal pH for ABE fermentation.

6.3.1 Dilute Phosphoric Acid Hydrolysis of Corn Stover

Corn stover consists of a variety of cellulosic components that cannot be used as a carbon source for the bacteria in the fermentation process. Two methods were considered for this necessary hydrolytic breakdown: alkaline pretreatment and acid pretreatment.

Alkaline pretreatment requires the addition of a strong base, typically sodium hydroxide. The combination of corn stover, water, and strong base is then heated and the cellulosic components of the stover are hydrolyzed to sugar (MacDonald et al. 1983).

Dilute acid pretreatment uses an acid at a very low, typically single digit, weight concentration of acid with the balance being water. Like alkaline pretreatment, this slurry is

typically heated. Dilute acid pretreatment does not necessitate that the catalytic acid be strong, and weak acids have facilitated successful sugar recovery (Um et al. 2003).

Both of these methods were successful at recovering glucose from cellulosic matter based on the literature reviewed by the team (Wang et al. 2016). Although acidic pretreatment had lower glucose yield (Wang et al. 2016) than alkaline pretreatment, the team's decision came down to the value of the waste stream derived from each method. Dilute acid pretreatment allows for a wide variety of acids to be chosen from, thus an acid with the ability to add value to the waste stream after the neutralization reaction could be selected. The team decided to move forward with dilute acid pretreatment, determining that a side stream with a valuable commodity product was of more value to the design than an increase in glucose availability.

Phosphoric acid was determined to be the ideal acid for this process given that the addition of phosphate to the waste is economically valuable. Kinetic data was found running the process at 100 °C, and a ratio of 1 part corn stover to 10 parts 3.76wt% dilute phosphoric acid would be ideal for our process (Gómora-Hernández et al. 2020). A glucose yield of 27.6wt% (weight glucose / weight milled corn stover) was determined (Avci et al. 2013). The kinetic information available necessitated that this be a batch process and as such the batch residence time was calculated to be 2.5 hours. Draining, cleaning, and filling of the reactor vessel were estimated to take approximately half an hour, resulting in an overall batch time of 3 hours. Batches were scheduled to be staggered to ensure that the continuous processes that follow are constantly being fed. A surge tank was also incorporated into the design to prevent any batch disruption from negatively impacting the downstream processes. To account for the high flow and to make the size of the batch reactors reasonable, each batch is broken into three reactors,

making three sets of three total (see Figure 6.3.1a). The reactor schedule for this setup can be seen in 6.3.1b.

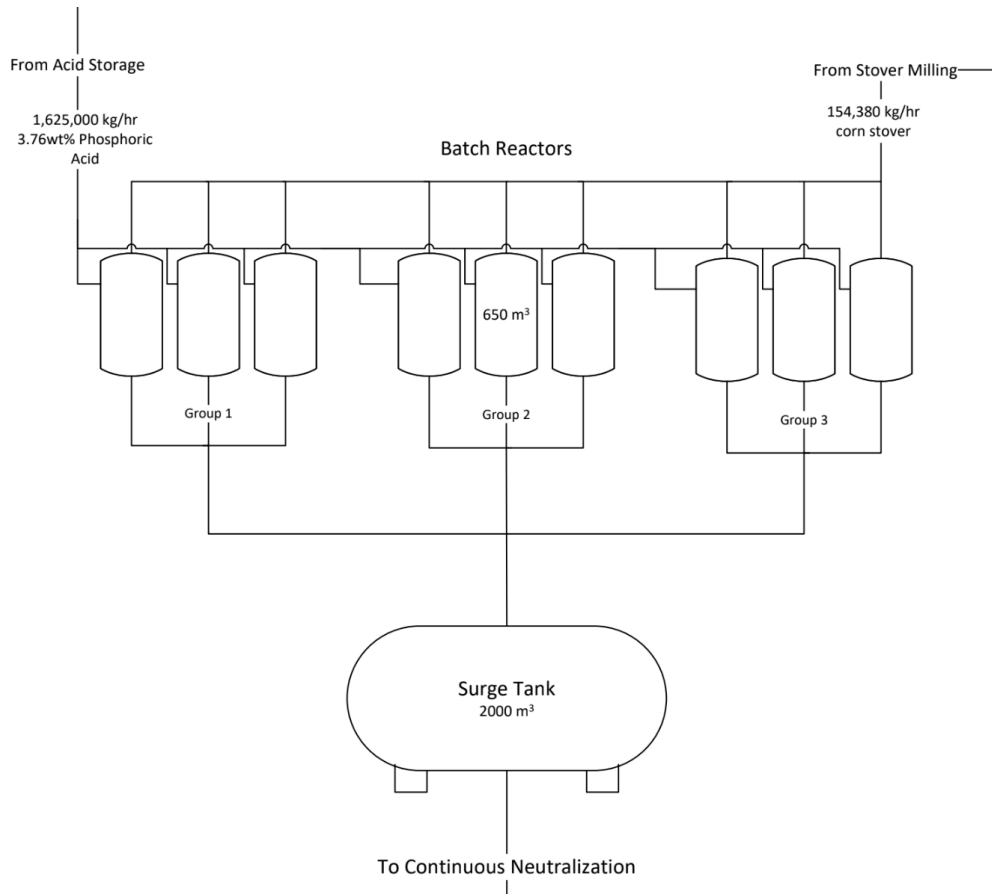


Figure 6.3.1a Reactor Layout for Dilute Acid Hydrolysis of Corn Stover

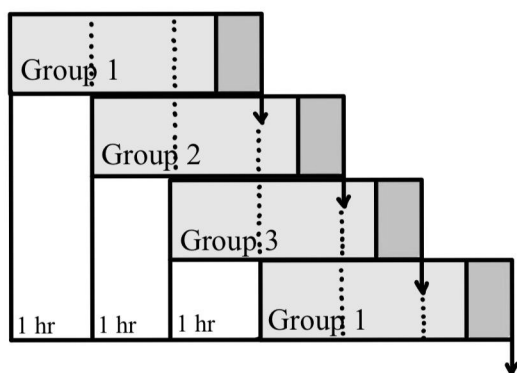


Figure 6.3.1b Hydrolysis Reactor Schedule

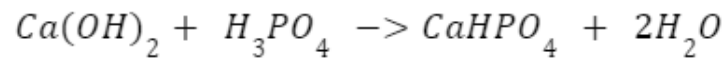
In order to get the temperature of each reactor to be 100 °C, the team analyzed ways of heating the reactor contents. Two methods were considered: heating the batch reactors after they are filled or heating the inlet streams before they are filled. Heating after filling was quickly determined to be too challenging, given that a jacketed reactor has a very small surface area to volume ratio to transfer heat over. Heating prior to filling was thus determined to be the optimal method; the dilute acid stream needed to be heated to a temperature of 103 °C to ensure that after mixing with dry corn stover at ambient temperature the final reactor temperature would reach 100 °C. Corn stover will not be heated on its own given that doing so poses a safety risk. Since the required temperature of the dilute acid stream being fed to the process is above the boiling point of the liquid the inlet stream will need to be kept above atmospheric pressure, chosen in this design to be 1.1 atm. Key details of each of the streams involved in this process can be seen in Table 6.3.1a.

Table 6.3.1a Compositions and Flow Rates for Dilute Acid Hydrolysis

Component	Stover [%] 25°C	Dilute Acid [%] 103°C	Hydrolysis Product [%] 100°C
Phosphoric Acid	0.00	3.76	3.40
Water	6.20	96.24	87.60
Dry Stover	93.80	0.00	0.00
Glucose	0.00	0.00	2.30
Stover Waste	0.00	0.00	6.70
Total Flow [kg/hr]	172,000	1,625,000	1,797,000

6.3.2 Neutralization of Phosphoric acid with Calcium Hydroxide

Before proceeding to the fermentation step, this acidic feed stream must be neutralized to the necessary pH for fermentation, which is 4.41 (Buehler & Mesbah 2016). The team decided to neutralize the stream with calcium hydroxide to produce an insoluble salt that would crash out of solution and be filtered out as a side stream that can be sold as a commodity. Dibasic calcium phosphate, or anhydrous calcium monohydrogen phosphate, is the most stable compound produced in the irreversible neutralization of phosphoric acid and calcium hydroxide at pHs lower than 4.8 (Dorozhkin 2011). The balanced reaction is shown below.



Equation 6.3.2a Neutralization Reaction

Given that the solution of acid and base is well mixed, this precipitation reaction, along with the dissociation of the constituent ions, occurs fast enough that these reactions can be considered to be at chemical equilibrium within the time scale of our process (Aspen Technology 1999). To model this, the team used an Aspen Plus flash calculation using the Electrolyte Wizard to account for all possible electrolyte reactions. Table 6.3.2.a depicts the electrolytes and dissociation reactions generated by the Electrolyte Wizard and included in the team's modeling.

Table 6.3.2a Electrolyte Wizard Inputs and Reactions

Electrolyte / Salt Species	Dissociation Reactions Considered
H2O	$\text{H}_3\text{PO}_4(\text{S}) + \text{H}_2\text{O} \rightleftharpoons \text{H}_3\text{O}^+ + \text{H}_2\text{PO}_4^-$
CA(OH)2	$\text{H}_3\text{PO}_4 \cdot 0.5\text{W}(\text{S}) + 0.5 \text{H}_2\text{O} \rightleftharpoons \text{H}_3\text{O}^+ + \text{H}_2\text{PO}_4^-$
H3PO4	$\text{H}_2\text{O} + \text{H}_2\text{PO}_4^- \rightleftharpoons \text{H}_3\text{O}^+ + \text{HPO}_4^{2-}$
CA+2	$\text{CAHPO}_4(\text{S}) \rightleftharpoons \text{CA}^{+2} + \text{HPO}_4^{2-}$
H3O+	$\text{H}_2\text{O} + \text{HPO}_4^{2-} \rightleftharpoons \text{H}_3\text{O}^+ + \text{PO}_4^{3-}$
CAOH+	$\text{CA}(\text{OH})_2(\text{S}) \rightleftharpoons \text{CAOH}^+ + \text{OH}^-$
CAHPO4	$\text{CAOH}^+ \rightleftharpoons \text{CA}^{+2} + \text{OH}^-$
CA(OH)2	$\text{CA}(\text{OH})_2 \rightarrow \text{CAOH}^+ + \text{OH}^-$
H3PO4*1/2W	$\text{H}_3\text{PO}_4 \cdot \text{W}(\text{S}) \rightleftharpoons \text{H}_3\text{O}^+ + \text{H}_2\text{PO}_4^-$
H3PO4	$2 \text{H}_2\text{O} \rightleftharpoons \text{OH}^- + \text{H}_3\text{O}^+$
H2PO4-	$\text{H}_3\text{PO}_4 + \text{H}_2\text{O} \rightleftharpoons \text{H}_3\text{O}^+ + \text{H}_2\text{PO}_4^-$
OH-	
HPO4-2	
PO4-3	

The solubility of CaHPO_4 at 25 °C is low, at 0.048 g/L (Dorozhkin 2011). The stream exiting dilute acid hydrolysis at 100°C needed to be cooled to 25 °C before neutralization for optimal insolubility (Ibrahim et al. 2017). The solid $\text{Ca}(\text{OH})_2$ feed stream for neutralization was also modeled to enter the neutralization tank at 25 °C. To model this reaction in Aspen, the corn waste and glucose from hydrolysis were neglected as input materials. The reaction simulation was run adiabatically at atmospheric pressure (1 atm). The stream table output with corn waste and glucose included is shown in Table 6.3.2b.

Table 6.3.2b Compositions and Flow Rates for Neutralization before Filtration

Component	Base [wt.%] 25°C	Dil Acid Hydrolysis Stream [wt.%] 25°C	Neutralization Product [wt. %] 31.7°C
H ₂ O	0.0%	87.5%	85.0%
Ca(OH) ₂	100.0%	0.0%	0.0%
H ₃ PO ₄	0.0%	2.8%	0.0%
CaHPO ₄	0.0%	0.0%	4.5%
Other Ions/Salts	0.0%	0.7%	0.0%
Corn Waste	0.0%	6.7%	6.4%
Glucose	0.0%	2.3%	2.3%
Total [kg/hr]	46,000	1,797,000	1,843,000

To ensure that the large solution volume is well mixed, the team assumed an approximate residence time of 10 minutes to determine the volume of reactor needed for continuous operation. With this assumption, this process requires a reactor volume of approximately 350 m³ (350,000 L). The process flow diagram around the neutralization reactor is shown in Figure 6.3.2a. The neutralized stream is filtered through a disk filter, where the solid waste stream is assumed to be 50 wt.% water. This solid waste stream, rich in corn waste and CaHPO₄, is to be a vital source of profit for the plant. One of calcium monohydrate phosphate's common uses is as a food additive for livestock. This, added with solid corn waste, makes a product suitable for a cattle food supplement. Table 6.3.2c shows the compositions of the neutralization product stream after filtration. Figure 6.3.2a depicts this neutralization and filtration step.

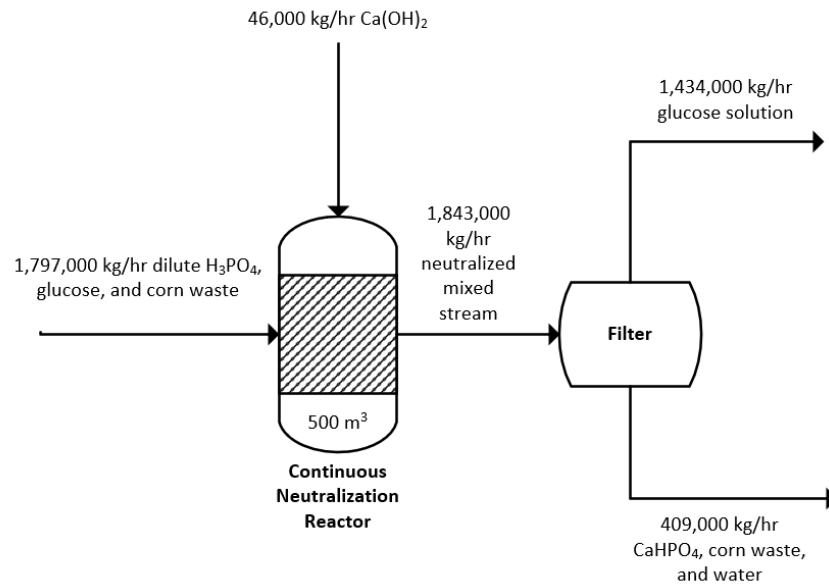


Figure 6.3.2a Neutralization Process Flow Diagram

6.3.3 Filter Design

A disk filter was selected for this process given its application to continuous processes while also having the lowest cost per unit area (Schweitzer 1979). This filter type was sized using correlations available in Perry's Handbook on page 18-85. The calculation for this value can be seen below in Figure 6.3.3. Values not calculated here but used in the calculation were provided in Perry's Handbook as part of the design process.

Maximum effective submergence = 0.28;

Maximum portion of the filter available for dewatering = 0.45

Scale up: On rate = 0.8, On area = 0.8, On discharge = 0.9 → scale up factor = 0.58

Cake thickness = 1.5cm (slightly larger than minimum)

$W = 20 \frac{\text{kg dry cake}}{\text{m}^2 * \text{cycle}}$ for that cake thickness

Form time = 1.20 min, so formation cycle time (CT_{form}) = $\frac{1.20 \text{ mins}}{0.28} = 4.29 \text{ mins}$

Using 50 wt% water, dry time = 0.02 min, so dry cycle time (CT_{dry}) = $\frac{0.02 \text{ mins}}{0.45} = 0.044 \text{ mins}$

$\frac{20 \frac{\text{kg}}{\text{m}^2 * \text{cycle}}}{4.29 \frac{\text{min}}{\text{cycle}}} * 60 \frac{\text{min}}{\text{hr}} * 0.58 = 162 \frac{\text{kg}}{\text{m}^2 * \text{hr}}$ design filtration rate

Taking into account actual flow rate → $409 \frac{\text{MT}}{\text{hr}} * \frac{1000 \frac{\text{kg}}{\text{MT}}}{162 \frac{\text{kg}}{\text{m}^2 * \text{hr}}} = 2500 \text{ m}^2 \text{ filter area}$

Figure 6.3.3a Calculation for Disk Filter Area

A mesh filter material was selected for use inside the disk filter machine for both durability and cost effectiveness.

6.4 Fermentation

The cornerstone of the production of biobutanol is the Acetone-Butanol-Ethanol (ABE) fermentation process. For this process, the team selected the bacteria *Clostridium acetobutylicum* ATCC824 as the means of sugar fermentation. This choice was made for several reasons. First, this particular strain of *C. acetobutylicum* is particularly well studied in the realm of ABE fermentation and kinetic data are readily available. Second, these bacteria are resistant to the toxic effects of ABE metabolites at low concentrations, making them a good candidate for a continuous fermentation. Third, these bacteria are proficient at producing a high concentration of butanol compared to other common choices for ABE such as *Pseudomonas aeruginosa* (Rao, Sathiavelu, & Mythili 2016). Lastly, these bacteria perform ABE fermentation anaerobically, which provides a significant benefit to the size at which the plant can operate. Eliminating concerns regarding oxygen mass transfer limitation provides the ability to operate at a larger scale while simplifying equipment design.

6.4.1 Main Reactor Kinetics

The team elected to utilize a continuous model for the fermentation process. Because all processes besides acid hydrolysis operate continuously, developing fermentation to operate continuously removes the need for large and costly intermediate storage tanks both upstream and downstream of the process. Furthermore, running the fermentation continuously allows more freedom to adjust input conditions if deviations from expected growth trends are observed, whereas this would lead to an increase in wastage in a batch process. Most importantly, the continuous nature of the fermentation prevents the accumulation of toxic metabolites. While *C. acetobutylicum* has higher tolerance for ABE metabolites than most bacteria, it is still affected by the buildup of fermentation products. This product toxicity would severely limit the productivity

of a batch process, as the bacteria create an environment they cannot survive in as the process progresses. Continuous operation allows steady state removal of these toxic products and maximizes the overall productivity of the *C. acetobutylicum* cells in the fermentation.

The kinetic model used by the team consisted of 19 ordinary differential equations (ODEs) (Table 6.4.1a) that couple the metabolic pathways within the *C. acetobutylicum* to metabolite concentrations such that approximate rates of reaction can be derived (Buehler & Mesbah 2016). Using these approximate metabolic rate of reaction ODEs, a general model is developed to predict the time-dependent concentration of Acetone, Butanol, and Ethanol generated in the fermentation from input glucose and biomass concentrations as well as the dilution ratio. Initial conditions for this system can be found on Table 6.4.1b.

Table 6.4.1a Ordinary Differential Equations for the Fermentation Model

Metabolite	Equations (Concentrations in mM)
Glucose	$\frac{d[G]}{dt} = -R_1 - R_x - D([G] - [G_{in}])$
Fructose 6-Phosphate	$\frac{d[F_{6P}]}{dt} = R_1 - R_2 - D[F_{6P}]$
Glucose 3-Phosphate	$\frac{d[G_{3P}]}{dt} = R_2 - R_3 - D[G_{3P}]$
Pyruvate	$\frac{d[Py]}{dt} = R_3 + R_4 - R_5 - R_6 - D[Py]$
Lactate	$\frac{d[Lac]}{dt} = R_5 - R_4 - D[Lac]$
Butyrate	$\frac{d[B]}{dt} = R_{14} - R_{13} - D[B]$
Biomass	$\frac{d[X]}{dt} = R_x - R_d - D[X]$
Carbon Dioxide	$\frac{d[CO_2]}{dt} = R_6 + R_{11} - D[CO_2]$

Adc	$\frac{d[Ad]}{dt} = r_{Ad} + r_{Ad}^+ H - D[Ad]$
AdhE	$\frac{d[Ah]}{dt} = r_{Ah} + r_{Ah}^+ H - D[Ah]$
Acetate	$\frac{d[A]}{dt} = R_7 - R_8 - D[A]$
Ethanol	$\frac{d[En]}{dt} = R_{10} - D[En]$
Acetoacetyl-CoA	$\frac{d[AaC]}{dt} = R_9 - R_8 - R_{12} - R_{13} - D[AaC]$
Acetoacetate	$\frac{d[Aa]}{dt} = R_8 + R_{13} - R_{11} - D[Aa]$
Butyryl-CoA	$\frac{d[BC]}{dt} = R_{12} + R_{13} - R_{14} - R_{15} - D[BC]$
Acetyl-CoA	$\frac{d[AC]}{dt} = R_6 + R_8 - R_7 - R_9 - R_{10} - D[AC]$
Acetone	$\frac{d[An]}{dt} = R_{11} - D[An]$
Butanol	$\frac{d[Bn]}{dt} = R_{15} - D[Bn]$
CtfA/B	$\frac{d[Cf]}{dt} = r_{Cf} - r_{Cf}^+ H - D[Cf]$

Table 6.4.1b Fermenter Conditions

Variable	Value
T (°C)	37
P (atm)	1
pH	4.41
V _{total} (m ³)	10,000
V _{filled} (m ³)	7,500

Given these conditions, the optimal dilution ratio was found to be 0.01 h^{-1} , which gave the highest product concentrations without washout occurring. Other metabolites generated in this fermentation such as butyrate and lactate were sent further downstream in the separation process with water, and many of the additional components considered by the model remain as intracellular waste and exit the reactor with the biomass. Any accumulated waste within the fermenters is removed at the end of each fermentation cycle and fed to a belt filter press prior to disposal, which was sized to process 20,300 kg of wet biomass an hour, and which can also be utilized to partially dry the leftover sludge between cycles.

In order to use this model, some simplifying assumptions were made. The most impactful of which is the assumption that all necessary nutrients required for cell growth are present in the cellulolytic feedstock. While data supports the presence of glucose and other major bacterial food sources, trace elements promoting growth may not be naturally occurring in the feed. This could negatively impact cell growth rates and could serve as an area of future research. The team also assumed that the production of carbon dioxide from the anaerobic fermentation alone would be sufficient to “blanket” the headspace in each primary fermenter, such that the fermentation conditions are and remain anaerobic.

6.4.2 Main Fermentation Reactor Design

The primary design constraint for these reactors, volume, comes from the dilution ratio determined in the Reactor Kinetics section. Dilution ratio is defined as total input flow rate divided by reactor volume. With our total input flow, this necessitates 138,675 m³ of working reactor volume. The team divided this requirement into 18 fermenters, each with a 10,000 m³ volume running around 75% full to allow for off gassing and foaming. However, 20 fermenters were considered into the final design to account for process leeway/maintenance. To mix the reactors, ten mixing eductors will be fitted to the bottom of the tank to mitigate settling. Additionally, each primary fermenter will be fitted with a biomass collection system such that the slurry left behind after each fermentation cycle can be removed. These fermenters will be steel panel tanks constructed on site due to their size. Based on the continuous nature of the process and the scale of the primary fermentation tanks, the team does not believe there is a need to supplement additional heat to keep the fermentation at 37 °C. Furthermore, the biological reactions that occur within the primary fermenters are neither strongly endothermic or exothermic, so there is no requirement for a cooling or heating jacket on the primary fermenters - temperature is expected to be maintained at 37 °C.

6.4.3 Seed Reactor Design

To achieve the 1 mM initial biomass concentration across all fermenters, each primary fermenter needs to be started containing 1720 kg of biomass. Since 18 of these fermenters run each 30 day cycle, 30,960 kg of biomass needs to be produced monthly. To meet this requirement, seven seed trains (as seen in the diagram in Figure 6.4.3a) will be used. The largest reactor in this seed train is 500 m³ and when maximally productive will generate 2.4 kg of biomass per m³ of working reactor volume (Buendia-Kandia et al. 2018). Growing cells from the

first inoculum to this point is projected to take around 5 days, meaning it could be repeated 4 times on a monthly basis. This would yield approximately 4800 kg biomass per month. To reach the necessary mass of 30,960 kg/month, 7 of these seed trains will be used. This represents an estimated production of 33,600 kg/month.

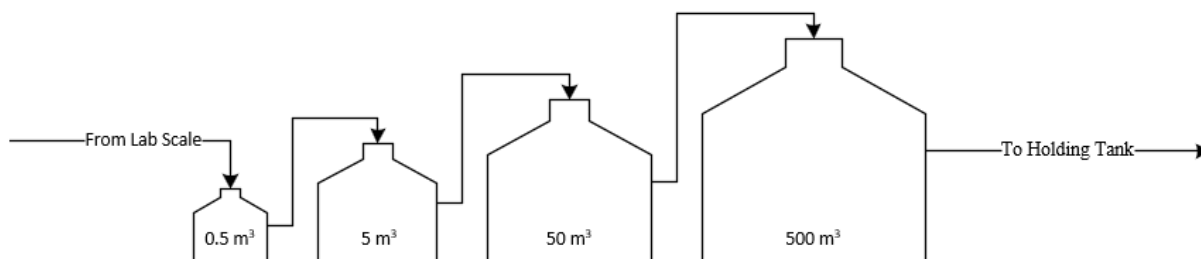


Figure 6.4.3a Seed Train Schematic

The lab scale growth of the biomass will take place in several 5 L and 50 L bioreactors. These will be operated as frequently as possible to create a working cell bank that will act as the inoculum of the seed train shown in Figure 6.4.3a. Seeding for the smallest 5 L bioreactor will come from a master cell bank of the *Clostridium acetobutylicum* ATCC824 purchased from a vendor. While detailed scheduling and procedures for this part of the plant were deemed to be out of scope for this project, their estimated economic costs are included in this report.

6.5 Separations

The separation block of this process consists of several unit operations that take the stream exiting fermentation and separate it into 99.99% purity butanol product and waste streams. The main unit operations of this process include hydrophobic pervaporation, decantation with accompanying recycle column, hydrophilic pervaporation, and a final column to separate butanol from acetone and ethanol (Figure 6.5a).

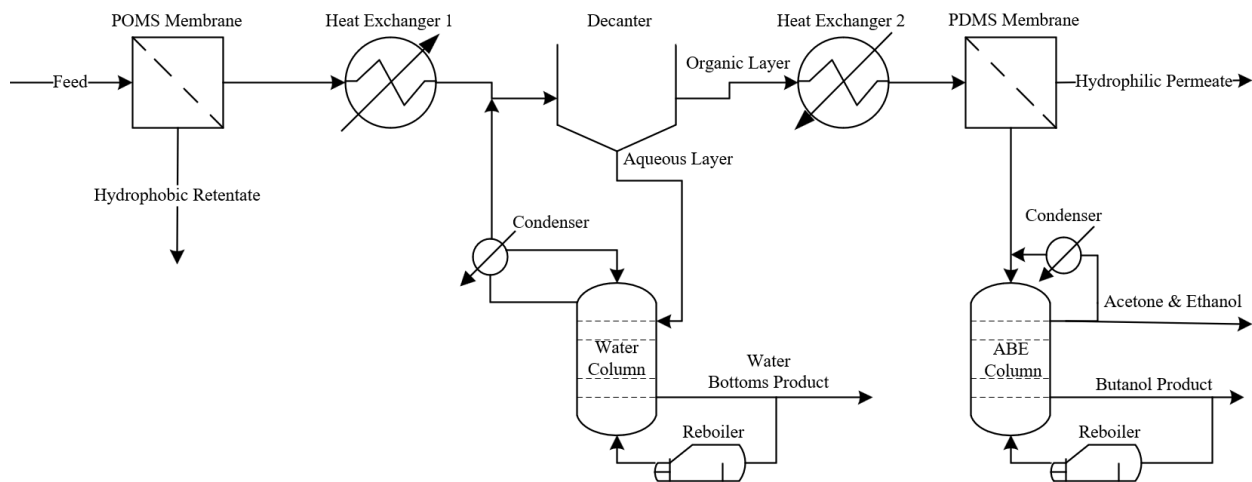


Figure 6.5a Simplified process flow diagram of separations block

Pervaporation, a combination of permeation and evaporation, is the passing of material along a filter, where the permeate side of the filter is held at much lower pressure than the feed side. Pressures for operation of this process generally fall within the range of 100 to 2500 Pa. For this process, 280 Pa was determined to be the ideal operating pressure for the permeate sides in all pervaporation units for the filter material (Kujawska et al. 2016). Feed sides were maintained at atmospheric pressure (101325 Pa). Changing membrane materials to allow for both hydrophilic and hydrophobic pervaporation enables increased selectivity to suit project needs. Since the streams exiting the permeates will be low-pressure vapors, vacuum pumping systems

are required to operate the pervaporation processes, and condenser/compressor equipment is necessary to return to liquid phase flow and atmospheric pressure. The novelty of this unit operation at an industrial scale allows the team to avoid complex azeotropic distillation while differentiating the project from others.

Distillation is necessary in two distinct places in our separation process. One column is required to effect a separation of acetone and ethanol from the butanol product. The other column is required to recover butanol lost in the aqueous phase of decantation while removing water from the system before later separations.

6.5.1 Hydrophobic Pervaporation

Hydrophobic pervaporation uses membranes that are more resistant to the permeation of water versus other organic materials produced in ABE fermentation. This design uses poly(octylmethyl siloxane), abbreviated POMS, as the filter material due to its ability to more selectively transport organic compounds as opposed to water (Knozokwa et al. 2021). Biological material in the influent stream cannot be passed by the filter, but can result in filter fouling, which can be reversed by using a water backwash for almost zero difference in performance as compared to unfouled filters (Liu et al. 2011). A material balance and process flow diagram are included on Figure 6.5.1. Table 6.5.1 denotes the associated flux values by material. Based on their low concentrations, and the later behavior of the species to isolate entirely in the aqueous layer of decantation and thus remove themselves from the process, lactate and butyrate species were assumed to be at negligible concentrations and were not considered in the filter process and subsequent unit operations.

Table 6.5.1a
Flux Values by Material for POMS Membrane (Knozowska et al. 2021)

Species	Flux Value (kg/m ² h)
Water	7.5
Acetone	0.6
Butanol	2.1
Ethanol	0.3

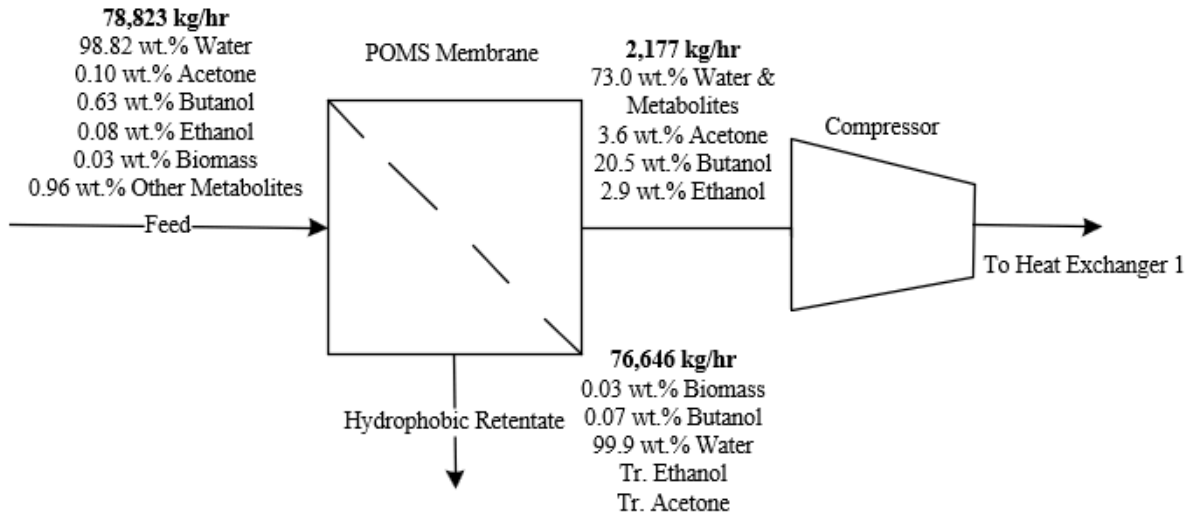


Figure 6.5.1a PFD and Stream Material Composition of Hydrophobic Pervaporation Unit

A total filter area of 212 m² is required per fermenter, which results in a process-wide scale of 3,816 m² of the POMS membrane required at operating capacity. Membrane thickness is recommended at 55 μm in order to balance the needs of structural resilience with mass transfer limitations. Based on the propensity for biological fouling reducing filter fluxes, it is recommended that each fermenter setup be outfitted with 283 m² of POMS membrane, such that they may be activated as sets of 70.7 m² to meet filter area requirements to effect separation while the remaining area undergoes backwash with water to remove fouling, giving a net total of 5,660 m² of filter area to completely outfit the process.

6.5.2. Decanter and Recycle Design

Following hydrophobic pervaporation, a two-phase separation coupled with a recycling apparatus are combined to effect a superior separation.

6.5.2.1 Phase Separation

The conditions of the flow exiting hydrophobic pervaporation combined with the recycle stream are such that the stream can form two immiscible liquids. This can be leveraged to effect a two-phase liquid/liquid separation into an organic-rich and an aqueous-rich phase. This separation occurs readily at 25 °C, and changes in temperature will affect miscibility properties (Zhou, Su and Wan 2014). Figure 6.5.2.1a shows the mass fractions of species in the mixture required for two phase separation to happen, where region I in the figure includes the two-phase heterogeneous mixture, while region II denotes the homogenous mixture. Figure 6.5.2.1a was referenced directly based on material compositions of the streams entering the decanter. Based on the material conditions exiting the hydrophobic pervaporation apparatus, the material stream is within the two-phase region. Compositions for these streams were then read off of the ternary phase diagram and applied to a material balance around the decanter. A ternary phase diagram was constructed in Aspen as well to confirm the readings off of this chart.

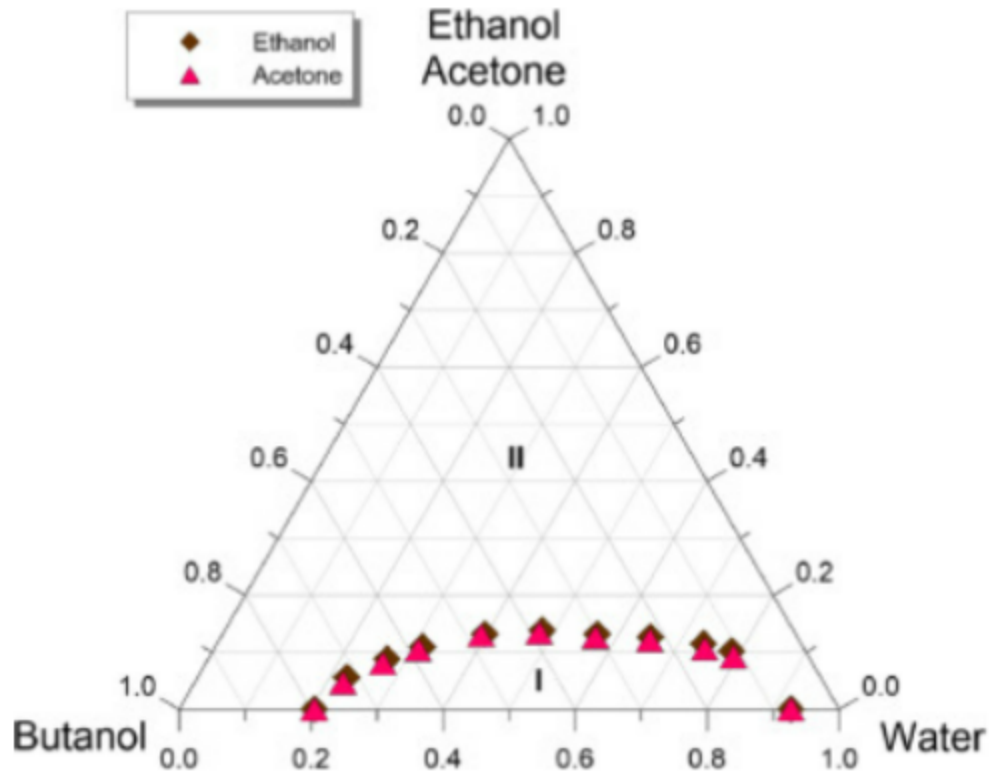


Figure 6.5.2.1a Ternary Phase Diagram (Knozowska et al. 2021)

6.5.2.2 Decanter Design

The separation of the two phase stream takes place in a decanter. A gravity decanter design was selected by the team, based on the ready separation of the two liquid layers and the low energy requirement of operating such a unit (Dimitrijević, Bösenhofer, and Harasek 2023). Gravity decanters, also known as settlers, use density differences in the immiscible phases in order to effect a separation, and then pull these different layers off based on their locations (Dimitrijević, Bösenhofer, and Harasek 2023). Figure 6.5.2.2a demonstrates how the gravity decanter would work in this process. The heavy phase would be the aqueous phase and the light phase would be the organic phase.

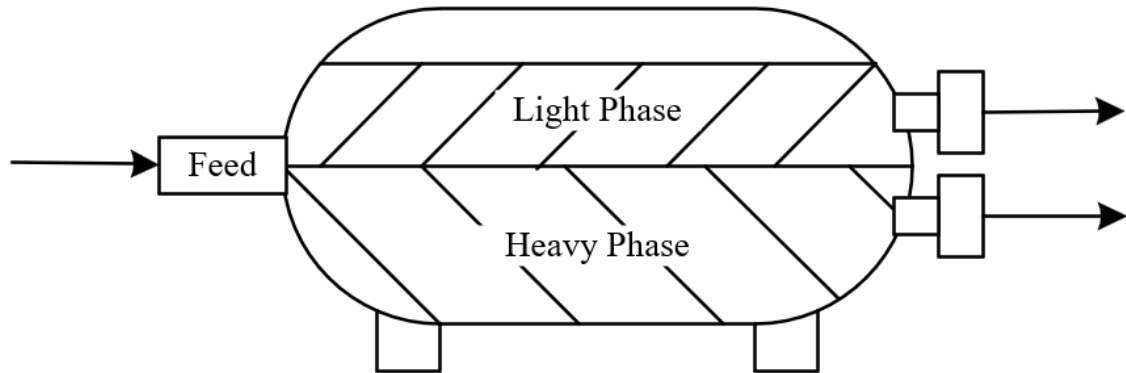


Figure 6.5.2.2a Example Design of Gravity Decanter

Sizing for the decanter was based on a 7 minute material phase-separation residence time (Stewart 2008). Based on the volumetric flow rate into the decanter and by employing a 60% fill fraction, which is in line with typical decanter design practices, the decanter will have a volume of 13.5 m³.

6.5.2.3 Recycle Column

In order to prevent an approximately 50% product loss in the aqueous phase after the decantation step, the team felt it was necessary to add a recycle stream to increase yield. While a typical recycle with a purge stream could have been viable, a column was used in order to prevent all butanol loss during the decanting step and remove excess water from the system.

All of the butanol will be recycled out of the top with acetone, ethanol, and some water, while only water comes out the bottom of the column. The tops product will be mixed with the outlet of the hydrophobic pervaporation and is then sent into the decanter.

The recycle column was designed in Aspen using the RadFrac modeling block. The column operates at atmospheric pressure with a reboiler temperature of 97.1 °C and a condenser temperature of 77.8 °C, with a heat duty of 80 MW and -76 MW, respectively. The input stream

is fed to the column on stage 8 and the total theoretical number of stages is 14. When the tray efficiency of 60% is accounted for, the actual number of stages is 25. The column spacing of 0.6096 meters means that the final height of the column is 15 meters. The column diameter is 5.7 meters total. The design and appropriate flow rates and compositions can be seen in Figure 6.5.2.3a. Table 6.5.2.3a summarizes the column sizing and energy specifications.

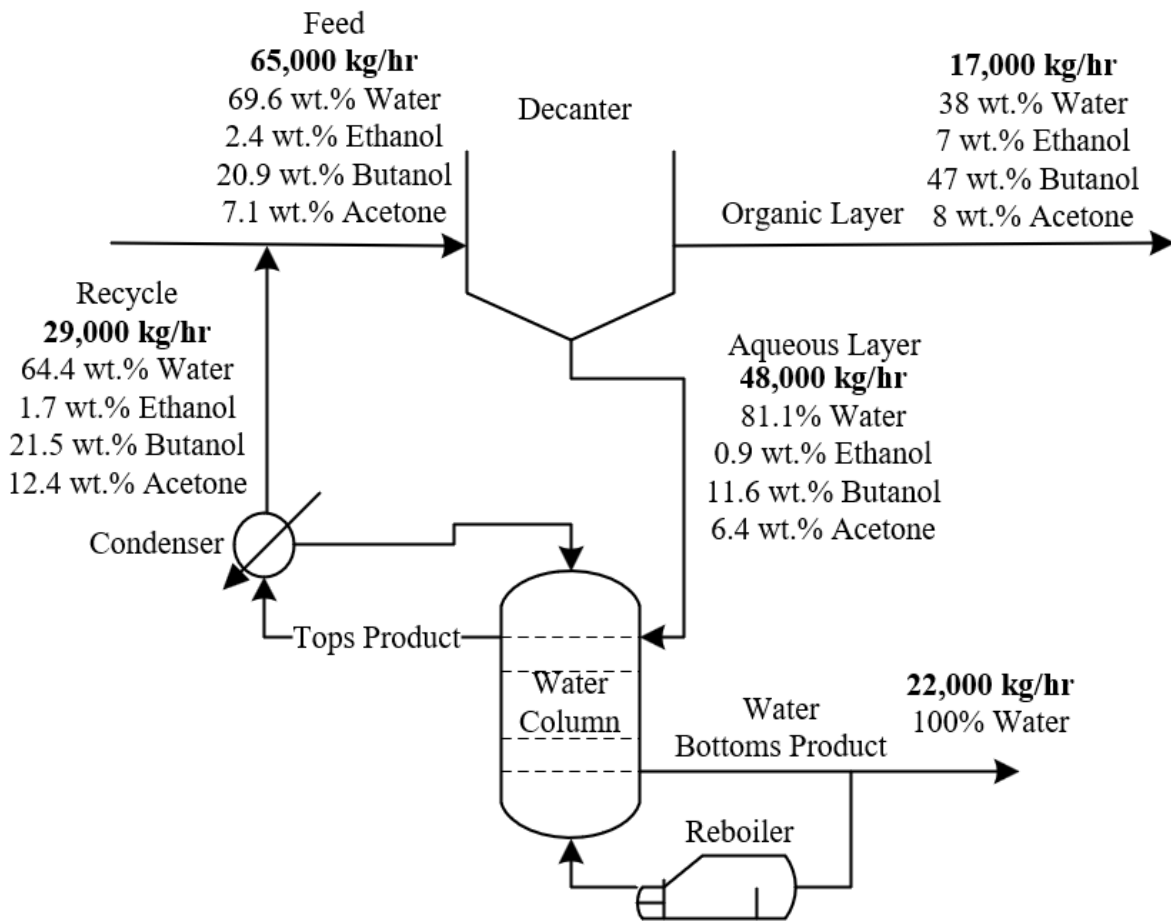


Figure 6.5.2.3a The Decanter Recycle Column

Table 6.5.2.3a
Recycle Column Sizing and Energy Specifications

Decanter Recycle Column Specifications	
Reboiler Duty	80 MW
Condenser Duty	-76 MW
Reboiler Temperature	97.1°C
Condenser Temperature	77.8°C
Diameter	5.7 m
Column Height	15 m
Tray Efficiency	60%
Number of Actual Stages	25

6.5.3 Hydrophilic Pervaporation

Hydrophilic pervaporation is used to extract water from the organic phase stream that is left over from the decantation unit. Cutting down on the water fed into the distillation process for recovering butanol and other commodities drastically reduces energy requirements of separation, and aids in obtaining marketable purities for the materials. Hydrophilic pervaporation will be accomplished using a PDMS/ceramic composite membrane. A composite membrane has two components: an active layer containing the material that primarily conducts material transfer, and a support layer that provides structure to the filter (Niemistö, Kujawski, and Keiski 2013). Here, the PDMS is the active layer and the ceramic forms the support structure (Liu, Wei and Jin 2014). The ceramic material is a combination of $\text{Al}_2\text{O}_3/\text{ZrO}_2$ tubes, and the PDMS layer is applied as a coating onto a ceramic network to form a thin active layer (Liu et al. 2011). The expected membrane thickness is 12 mm. A total filter area of 11,000 m^2 will be necessary to effect the separation at the process scale. Figure 6.5.3 shows the PFD and material streams found within the hydrophilic pervaporation unit, and Table 6.5.3 denotes literature flux values associated with the PDMS/ceramic composite filter membrane.

Table 6.5.3a
Flux Values for Material Across PDMS/Ceramic Composite
Membrane (Liu et al. 2011)

Species	Flux Value (kg/m ² h)
Water	0.59
Acetone	0.03
Butanol	0.05
Ethanol	0.01

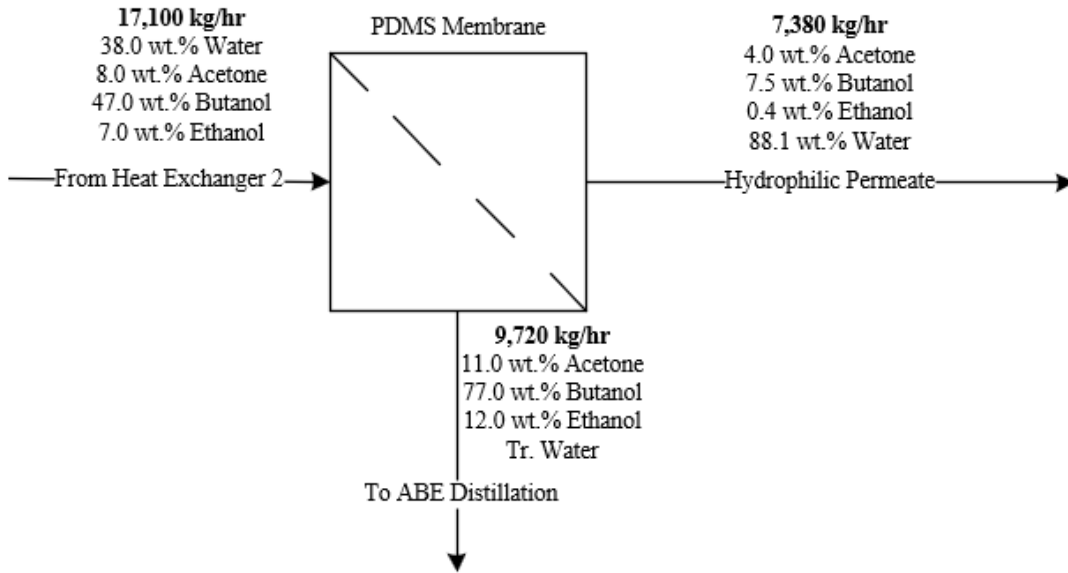


Figure 6.5.3a PFD with Stream Material Composition of Hydrophilic Pervaporation Unit

6.5.4 ABE Column

Coming out of hydrophilic pervaporation, the mixed stream has a composition of 11.0 wt. % acetone, 77.0 wt.% butanol, 12.0% wt.% ethanol, and trace water (<1 wt.%). Separation of butanol from ethanol and acetone becomes easier due to the lack of a limiting butanol-water azeotrope. The general process flow diagram for this column is shown in Figure 6.5.4a.

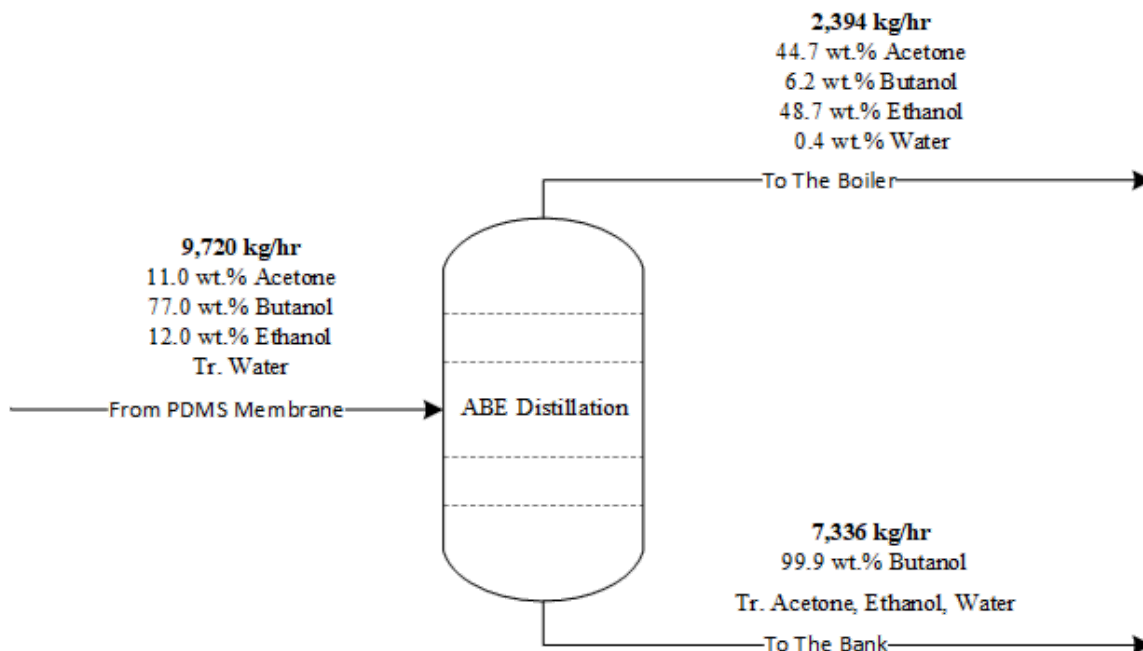


Figure 6.5.4a ABE Distillation Column PFD

To determine the feed temperature and operating pressure of the column, the team created a vapor pressure versus temperature graph with all four components—acetone, ethanol, butanol, and water (Figure 6.5.4b). Because there was such a low composition of water in the feed stream, the team chose an operating point between acetone/ethanol and water/butanol to achieve a desired separation between components, allowing some water to stay with the butanol rich bottoms stream. The temperature of the feed was thus 90 °C and the operating pressure was 1 atm. The distillation process was modeled in Aspen Plus using the NRTL property method (Pudjiastuti et al. 2021).

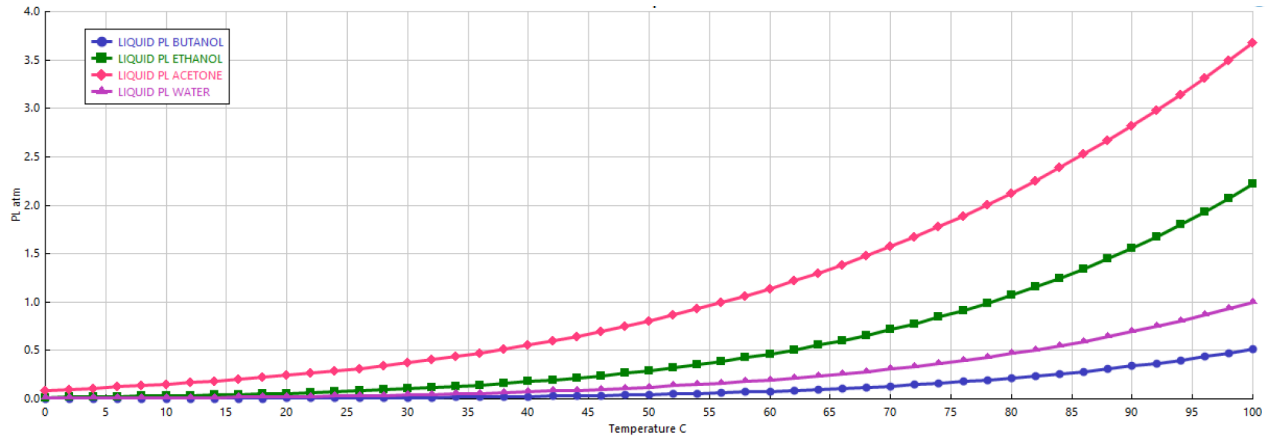


Figure 6.5.4b ABE & Water Vapor Pressure versus Temperature

After this separation, the purity of butanol (99.99 wt.%) reaches the ASTM standard specification for butanol for blending with gasoline, which requires at least a 96 wt.% purity of butanol and maximum water content of 1% (*Standard Specification for Butanol for Blending with Gasoline for Use as Automotive Spark-Ignition Engine Fuel*, 2021). The team has decided to burn the tops product of 44.7 wt.% acetone, 6.2 wt.% butanol, and 48.7 wt.% ethanol, and 0.4% water due to economic considerations outlined in Section 6.7.

To achieve this level of separation, there were specific column size and energy requirements shown in Table 6.5.4a. To determine the true height of the column and actual number of stages, the team used the O'Connell correlation for tray efficiency. This is explained in the following section (Section 6.5.5). From this correlation, the number of stages needed was 18, with the feed on tray 4.

Table 6.5.4a ABE Column Sizing and Energy Specifications

ABE Distillation Column Specifications	
Reboiler Duty	2.4 MW
Condenser Duty	-2.3 MW
Reboiler Temperature	118°C
Condenser Temperature	64°C
Diameter	1.3 m
Column Height	11 m
Tray Efficiency	76%
Number of Actual Stages	18

6.5.5 O'Connell Correlation

The O'Connell correlation takes into account some of the nonideal behavior of compounds during separation in a distillation column. The tray efficiency can be calculated using the equation in Figure 6.5.5 (Duss 2018). The viscosity of the mixture and the relative volatility are used to predict the ratio of theoretical stages to actual stages (i.e. tray efficiency).

$$\eta_{section} = 0.503(\mu_L \alpha)^{-0.226}$$

Equation 6.5.5a The O'Connell Correlation

For the calculation of the mixture viscosity, the team used an average of the component properties weighted according to the composition of the incoming feed stream. The relative volatility was the ratio of the light key and heavy key vapor pressures. The ABE column was found to have an efficiency of 76% and the recycle column had an efficiency of 60%.

6.6 Auxiliary Equipment

6.6.1 Heat Exchangers

In order to adjust temperature between the different unit operations within this process, many heat exchangers were required. It was decided that the best design would be a countercurrent, shell-and-tube heat exchanger, given that they are both widely commercially available and efficient.

The required area of heat transfer was calculated using the equation presented in Equation 6.6.1a. In this equation, A is the area of heat transfer to be solved for, while Q is total heat transferred, U is the heat transfer coefficient, and the temperatures present the inlet and outlet temperatures of the two countercurrent streams.

$$Q = U_o * A_o * \Delta T_{lm} = U_o * A_o * \frac{(T_{Hin} - T_{Cout}) - (T_{Hout} - T_{Cin})}{\ln\left(\frac{T_{Hin} - T_{Cout}}{T_{Hout} - T_{Cin}}\right)}$$

Equation 6.6.1a Heat Exchanger Equation

For the heat exchangers that were increasing the temperature of the tube-side fluid, 3 bar gauge saturated steam was used in the shell. For the exchangers that were decreasing the temperature of the tube-side fluid, cooling water at 24 °C was used in the shell. Estimated heat transfer coefficients that took into account the fluids on both the shell side and the tube side were found in Perry's Handbook. The 3 bar steam heat exchangers were found to have a heat transfer coefficient of 4,542 W/m²K and the cooling water exchangers had a heat transfer coefficient of 225 W/m²K.

The total heat requirements for the heat exchangers (Q) that were not modeled using ASPEN, which includes those heat exchangers that did not model a phase change or that were

immediately following compression processes, was found for each scenario using the equation presented in Equation 6.6.1b. In this equation, m is the mass flow rate of the stream, c is the specific heat capacity of the stream, and ΔT is the temperature change of the stream through the heat exchanger.

$$Q = m * c * \Delta T$$

Equation 6.6.1b The Total Heat Transfer Requirement Equation

The areas were solved using the two aforementioned equations and they are presented in a cumulative Table within the Economics section of this report (Section 7.1). These areas will be spread out over the many tubes of the shell-and-tube heat exchangers.

Two other heat exchangers (condensers) needed in the process were designed in ASPEN on account of the unusual nature of their input streams and the phase change requirement. These are located after the compressors in pervaporation (See section 6.6.4). The team found it more convenient to concurrently design these condensers with the compressors in Aspen as opposed to separately doing the aforementioned hand calculations. To design these heat exchangers in Aspen, the cooler block was used. Required inputs for this block include the inlet and outlet steam temperatures and amount of material stream (kg/hr). Aspen assumes a shell and tube single pass model and returns a required area and amount of cooling water needed. Both metrics were used in final pricing of heat exchangers, (see Section 7.1).

6.6.2 Pumps

Throughout the plant, pumps were designed using a base assumption of no significant elevation change and that they are made of “construction compatible” materials to accommodate the fluids they handle. There are 20 locations where pumps were designed for the biobutanol

plant. To account for sudden pump failure or maintenance, a spare pump was designed for every process critical pump in the system. More complex pumps were designed in Aspen; details of these pumps can be seen in the Economics section. A few more simple pumps were designed using Peters et al., (2003). In Peters et al. (2003), capacity factor in $\text{m}^3/\text{s} * \text{kPa}$ was needed to estimate the purchase cost per centrifugal pump, and capacity in m^3/s was needed to determine purchase cost per reciprocating pump. This cost calculation is further defined in the economics section (Section 7).

For centrifugal pumps, flow rate capacity in kg/hr was divided by the density of the most abundant feed material, and divided by 3,600 s to get a value in m^3/s which can then be multiplied by 1000 Pa, which is the Peters et al. figure's scaling factor to get capacity factor. Capacity factor is required to read off the correlation curve and find purchased pump cost (see Section 7.1).

For reciprocating pumps, flow rate in kg/hr was multiplied by the density of the most abundant feed material and then divided by 3,600 s to get capacity in m^3/s . Power (P) in kW was determined for each pump using Equation 6.6.2a, where q is flow rate m^3/h , ρ is density in kg/m^3 , g is gravity in $9.81 \text{ m}/\text{s}^2$, and h is differential head in meters (*Pump Power Calculator* 2023). It was assumed that there were no significant elevation changes, with 150 m of head used. Frictional losses were assumed to be 0.5 atm in pipes, and 0.5 atm for control valves on centrifugal pumps. Frictional losses were accounted for in the differential head value.

$$P = \frac{q * \rho * g * h}{3.6 \times 10^6}$$

Equation 6.6.2a Pump Power Equation

6.6.3 Conveyors

Four conveyors are required in the first half of the plant to move large amounts of at least 50 wt. % solid material, all of which can be found in Table 6.6.2b. One assumption made was that the linear feet of conveying for each system was about 150. Screw and belt conveyors were selected for specific advantages and to accommodate certain flow rates. According to Peters et al. (2003), screw conveyors accept fibrous or dusty solids, have a maximum bulk capacity of $0.08 \text{ m}^3/\text{s}$, and conveying speed of 0.1 m/s . Using Figure 12-60 in Peters et al. (2003), a screw conveyor that conveys about 150 feet has a diameter of 0.23 meters, and power requirement of 0.75 kW. Purchase and operating cost can be generated from Figure 12-60 in Peters et al. (2003), but will be discussed later in more detail in Section 7.1. According to Peters et al. (2003), belt conveyors can transport large fibrous capacities over long distances at relatively low cost, with a max bulk capacity of $2.0 \text{ m}^3/\text{s}$, and conveying speed of up to 5 m/s . To accommodate larger carrying capacities, Table 12-16 in Peters et al. (2003) gives design data for 45° troughed belt conveyors. Belt width can be determined by dividing stream flow rate by 3,600 s to find belt capacity in kg/s. To determine belt speed and subsequent power requirement, conveying distance of 150 feet was translated to meters, and divided by the lowest belt speed available to get conveying time in seconds. The plant runs on a kg/hr basis, and therefore if the conveying time is less than 10 minutes, the minimum belt speed of 0.51 m/s was considered usable.

Table 6.6.3a Preliminary conveyor belt details, with costs associated in Section 7.1

Conveyor Location	Flow Rate (kg/hr)	Type	Belt Width (m)	Power Requirement (kW)
To Milling	181,000	Belt	0.51	1.9
To Acid Pretreatment	172,000	Belt	0.51	1.9
To Feed Supplement Storage	409,000	Belt	0.51	3.72
From Ca(OH) ₂ Storage	46,000	Screw	0.23	0.75

6.6.4 Compressors

Pervaporation uses four-stage compressors at each membrane, where the inlet end of the compressor is held at the operating 280 Pa to induce vapor permeance of the membranes, and the outlet end is at atmospheric conditions. In both cases, compressors were coupled with a condenser and pump, which were able to output liquid streams after their operation. Compressors were assumed to have polytropic and isentropic efficiencies of 0.9, and were simulated using the polytropic ASME model.

The first compressor is the hydrophobic pervaporation compressor. The specifications for outlet stream conditions are strict, owing to the requirement for a two-phase separation in the following decantation step. A four-stage compressor setup was used, with a compression ratio of four (defined as discharge pressure over inlet pressure). The final pressure of the stream exiting the compressors was 0.707 atm. Compressor design was done using the MCOMPR unit operation in ASPEN with inlet and outlet streams at conditions described in Fig. 6.5.1a. An accompanying single-pass shell-and-tube condenser was also modeled to induce phase transition to liquid. This was followed by a liquid pump sized to raise the pressure of the outlet steam to 1 atm for downstream use in the decantation vessel to meet the requirements of two-phase separation as detailed previously.

The second compressor is the hydrophilic pervaporation compressor. Since the permeate of this membrane is a waste stream, thermodynamic constraints are lower than with the hydrophobic pervaporation step. A four-stage compressor setup was used, with a compression ratio of four. The final pressure of the stream exiting the compressors was 0.707 atm. Compressor design was done using the MCOMPR unit operation in ASPEN with inlet and outlet streams at conditions described in Fig. 6.5.3a. An accompanying single-pass shell-and-tube condenser was also modeled to induce phase transition to liquid. This was followed by a liquid pump sized to raise the pressure to 1 atm for use of the permeate stream as a water source for recycling.

A summary of the compressors, and subsequent ancillary equipment pertaining to compression processing, sizing, power requirements, and pricing information can be found in Section 7.1 of this report.

7. Economics

7.1 Detailed Equipment Pricing

The following tables show each specific piece of equipment in the process with key features, operating requirements, and costs (both operating and capital). Total operating costs are outlined in Section 7.4.

Table 7.1a details the conveyor costs. The conveyors were priced using Peters et al. (2003), by using conveying distance and conveyor type and width to locate purchase cost based on the correlation curve.

Table 7.1b details the pump costs throughout the plant. As detailed in Section 6.6.2 on pumps, capacity factors were calculated from flow rates. These capacity factors were ultimately used to find the pumps' capital costs from a correlation curve (Peters et al., 2003). To determine pump operating cost, the team used the energy requirement calculated using Equation 6.6.2a (in kW), the price of electricity (\$0.1/kWh), and the total operational hours for the year (7200 hrs). More complex pump designs associated with the compressor steps, such as pumps E-P02 and E-P07, were designed and priced in Aspen.

Table 7.1c details tank costs. Tank pricing was based on material and volume of the tank. The prices were found via Peters et al. (2003), with pricing dependent upon size of tank and material of construction desired.

Table 7.1d details heat exchanger pricing. The capital cost of each heat exchanger was determined based on the area required, as calculated in Section 6.6.1. The team compared these areas to a cost curve from Peters et al. (2003), that predicted the price of carbon steel heat exchangers based on required area. Once the amount of steam or cooling water needed was determined (Section 6.61), operating costs were determined based on the common prices of 3 bar

(low pressure) steam and 24°C cooling water outlined in Section 7.4. Like in pump design, other more complex or large material throughput heat exchangers (C-HE01, E-HE02, E-HE04), were designed in Aspen due to capital cost pricing being beyond the cost curves found in Peters et al., (2003), or their associations with compressors concurrently designed in Aspen.

Table 7.1e details the costs of the reactors in the plant, including acid pretreatment and fermentation reactors. Reactors found outside of the fermentation process were priced using Humbird et al. (2017). Eductors and the belt filter press included in the fermentation were priced based on currently available equipment capable of satisfying process requirements. Primary fermentation tanks were priced based on the same capital cost curve as the storage tanks found in Peters et al., (2003). However, because the team was unable to find a cost curve that explicitly priced tanks of this large a volume, the cost per liter volume was calculated for the largest capacity on the curve and that quantity was multiplied by the fermenter volume to extrapolate the cost for these tanks.

Table 7.1f details costs associated with distillation columns. These columns were priced in Aspen using the Process Economic Analyzer feature based on column sizing. The efficiency of the column was factored into this analysis, given that it affected the number of trays needed and thus the size of the columns. The operating costs associated with these columns were also priced using Aspen's Economic Analyzer, which accounted for reboiler and condenser steam and cooling water costs.

Table 7.1g details the miscellaneous separations unit operations that needed associated pricing. These include the pervaporation filters, the decanter, and the disk filter required for corn waste separation. The decanter was priced as a tank, for which the pricing process was described above. The pervaporation filters were priced using size correlations for membrane filters found

in Peters et al. (2003), with modification applied based on the material of the membrane. The disk filter area size was used to determine the price using the same method as described for the pervaporation membranes.

Table 7.1h outlines the pricing, power, and pressure information for the two compressors needed in the pervaporation processes. The operating and capital costs were found using Aspen's Process Economic Analyzer. The costs presented here were ultimately based on material flow amount and operating conditions inputted.

Table 7.1i briefly summarizes the calculated capital and operating costs associated with the milling block from the beginning of the process. Using Wilson, (2011), capital cost for a hammer mill grinding biomass for ethanol conversion was based on a factor of 0.25 times ton of stover fed, with operating costs based on a factor of 0.7 times ton of stover fed.

Table 7.1a Conveyor Capital and Operating Cost Information

Conveyor Location	Stream label	Flow Rate (kg/hr)	Type	Belt Width (m)	Power Requirement (kW)	Capital Cost (USD)	Operating Cost (USD/year)
To Milling	A-S01 & A-S02	181,000	Belt	0.51	1.9	\$199,000	\$1,368
To Acid Pretreatment	B-S03	172,000	Belt	0.51	1.9	\$199,000	\$1,368
To Feed Supplement Storage	C-S08	409,000	Belt	0.51	3.72	\$238,800	\$2,678
From Ca(OH) ₂ Storage	C-S06	46,000	Screw	0.23	0.75	\$99,500	\$540

Table 7.1b Pump Capital and Operating Cost Information

Pump Location	Pump Label(s)	Number of Pumps (duplicated for maintenance security)	Type	Material	Total Power Requirement per pump (kW)	Capital Cost (USD)	Operating Cost (USD/year)
From H ₃ PO ₄ Storage	A-P01	2	Reciprocating	316 Stainless Steel	11.20	\$23,900	\$8,064
From H ₃ PO ₄ Dilution Tank	C-P01	2	Centrifugal	API-610 Cast Steel Casing	221.40	\$98,600	\$159,408
From Hydrolysis Reactors	C-P02 through C-P05	8	Centrifugal	API-610 Cast Steel Casing	499.92	\$1,578,400	\$278,928

Pump Location	Pump Label(s)	Number of Pumps (duplicated for maintenance security)	Type	Material	Total Power Requirement per pump (kW)	Capital Cost (USD)	Operating Cost (USD/year)
From Neutralization	C-P06	8	Centrifugal	API-610 Cast Steel Casing	251.10	\$190,500	\$278,928
To Fermentation after filtration	C-P07	2	Centrifugal	316 Stainless Steel	250.00	\$72,000	\$180,000
Seed Pump 1	D-P22 through D-P28	14	Centrifugal	Cast Iron	1.26	\$840	\$6,350
Seed Pump 2	D-P29 through D-P35	14	Centrifugal	Cast Iron	12.56	\$3,500	\$63,302
Seed Pump 3	D-P36 through D-P42	14	Centrifugal	316 Stainless Steel	125.56	\$252,000	\$632,822
Output Pump from Seed Fermentation	D-P01	2	Centrifugal	Cast Iron	627.82	\$72,000	\$452,030
Output Pump from Primary Fermenters	D-P02 through D-P21	40	Centrifugal	316 Stainless Steel	21.53	\$720,000	\$310,000
From Compressor E-C01	E-P02	2	Centrifugal	API-610 Cast Steel Casing	1.37	\$747,600	\$33,552
From Mixer to Decanter 1	E-P03	2	Centrifugal	API-610 Cast Steel Casing	67.24	\$22,000	\$37,512
From Decanter (Organic Layer)	E-P05	2	Centrifugal	API-610 Cast Steel Casing	57.92	\$15,800	\$32,328

Pump Location	Pump Label(s)	Number of Pumps (duplicated for maintenance security)	Type	Material	Total Power Requirement per pump (kW)	Capital Cost (USD)	Operating Cost (USD/year)
From Decanter (Aqueous Layer) Water Bottoms	E-P04	2	Centrifugal	API-610 Cast Steel Casing	63.51	\$19,600	\$35,424
Product From Recycle Column	E-P08	2	Centrifugal	API-610 Cast Steel Casing	57.92	\$16,000	\$32,328
From Compressor E-C02	E-P07	2	Centrifugal	API-610 Cast Steel Casing	0.25	\$171,600	\$32,904
From Hydrophilic Retentate to ABE Column	E-P06	2	Centrifugal	API-610 Cast Steel Casing	54.56	\$14,200	\$30,456
Hydrophobic Retentate Material	E-P01	2	Centrifugal	API-610 Cast Steel Casing	388.02	\$316,000	\$216,504
Water Recycle to Phosphoric Acid Dilution Tank	E-P10	8	Centrifugal	API-610 Cast Steel Casing	192.00	\$207,000	\$45,430
Pump to Butanol Storage	E-P09	2	Reciprocating	316 Stainless Steel	0.95	\$23,900	\$684
Pump to Furnace	E-P11	2	Reciprocating	316 Stainless Steel	0.27	\$8,800	\$194

Table 7.1c Tank Capital Cost Information

Tank Description	Tank Label(s)	Number of Tanks	Volume (m³)	Material	Capital Cost (USD)
Corn stover grain bins	A-T01 through A-T47	47	85,000	Tensile Steel	\$117,500,000
75 wt.% Phosphoric Acid Storage Tank	A-T48	1	30,000	316 Stainless Steel	\$2,289,200
Acid Dilution Tank	C-T01	1	300	316 Stainless Steel	\$613,800
Post Hydrolysis Batch Surge Tank	C-T02	1	2,000	316 Stainless Steel	\$4,529,800
Animal Feed Supplement Storage Tank	A-T50 through A-T70	21	85,000	Tensile Steel	\$52,500,000
Post Seed Fermentation Surge Tank	D-T01	1	2,000	Carbon Steel	\$108,000
Butanol Storage Tank	A-T71	1	6,000	Carbon Steel, floating roof	\$230,200
Ca(OH) ₂ Storage Tank	A-49	1	17,000	Carbon Steel	\$160,000

Table 7.1d Heat Exchanger Capital and Operating Cost Information

Heat Exchanger Description	Label	Material	Area Required (m²)	Utility	Capital Cost (USD)	Operating Cost (USD/year)
Before Hydrolysis	C-HE01	Carbon Steel	495	Steam (3 bar)	\$1,070,800	\$65,624,800
Before Neutralization	C-HE02	Carbon Steel	8,010	Cooling water	\$27,860	\$2,651,100
Before Fermentation	D-HE01	Carbon Steel	1,316	Steam (3 bar)	\$20,298	\$2,027,000
Before Hydrophobic Pervaporation	E-HE01	Carbon Steel	4,202	Steam (3 bar)	\$157,600	\$8,703,800
Condenser with Compressor E-C01	E-HE02	Carbon Steel	2,965	Cooling water	\$732,000	\$419,000
Before Hydrophilic Pervaporation	E-HE03	Carbon Steel	59	Steam (3 bar)	\$5,400	\$1,888,200
Condenser with Compressor E-C02	E-HE04	Carbon Steel	616	Cooling water	\$159,200	\$87,100

Table 7.1e Reactor Capital Cost Information

Reaction Process	Reactor Label(s)	Number of Reactors	Volume (m³)	Material	Capital Cost (USD)
Hydrolysis	C-R01 through C-R09	9	650	316 Stainless Steel	\$15,822,000
Neutralization	C-R10	1	500	316 Stainless Steel	\$1,353,000
Seed Fermentation Step 1	D-SF01	7	0.5	316 Stainless Steel	\$35,000
	D-SF05				
	D-SF09				
	D-SF13				
	D-SF17				
	D-SF21				
	D-SF25				
Seed Fermentation Step 2	D-SF02	7	5	316 Stainless Steel	\$231,000
	D-SF06				
	D-SF10				
	D-SF14				
	D-SF18				
	D-SF22				
	D-SF26				
Seed Fermentation Step 3	D-SF03	7	50	316 Stainless Steel	\$490,000
	D-SF07				
	D-SF11				
	D-SF15				
	D-SF19				
	D-SF23				
	D-SF27				

Reaction Process	Reactor Label(s)	Number of Reactors	Volume (m ³)	Material	Capital Cost (USD)
Seed Fermentation Step 4	D-SF04	7	500	316 Stainless Steel	\$1,400,000
	D-SF08				
	D-SF12				
	D-SF16				
	D-SF20				
	D-SF24				
Primary Fermentation	D-F01 through D-F20	20	10,000	316 Stainless Steel	\$200,000,000

Table 7.1f Distillation Column Capital and Operating Cost Information

Column Description	Column Label	Stages	Total Power Requirement (kW)	Capital Cost (USD)	Operating Cost (USD/year)
Decanter Recycle Column	E-COL01	25	156	\$4,017,000	\$11,347,420
ABE Separations Column	E-COL02	18	4.7	\$2,454,830	\$617,040

Table 7.1g Other Separations Process Capital Cost Information

Other Separations Description	Label	Number of units	Membrane area (m²)	Membrane Material	Volume (m³)	Capital Cost (USD)
Hydrophobic pervaporation units	E-PV01 through E-PV18	18	281	Hollow fiber	--	\$167,800
Hydrophilic pervaporation	E-PV19	1	11000	Ceramic	--	\$28,457,700
Disk Filter	C-DF01	1	2500	Plate and Frame	--	\$1,493,000
Decanter	E-D01	1	---	---	13.5	\$30,800

Table 7.1h Compressor Capital and Operating Cost Information

Label	Flow Rate (kg/hr)	Type	Inlet Pressure (atm)	Outlet Pressure (atm)	Power Requirement (kW)	Cooling Duty (kW)	Capital Cost (USD)	Operating Cost (USD)
E-C01	39,186	Centrifugal Motor	0.003	0.707	11,809	-9735	\$3,000,000	\$5,101,488
E-C02	7,380	Centrifugal Motor	0.003	0.707	2,602	-2171	\$1,500,000	\$1,124,064

Table 7.1i Hammer Mill Capital and Operating Cost Information

Equipment Description	Label	Number of units	Capital Cost (USD)	Operating Cost (USD/yr)
Hammer Mill	B-HM01 & B-HM02	2	\$359,533	\$1,005,572

7.2 Total Plant Capital Cost

A summary table grouping major equipment and their overall costs are described in Table 7.2a. It should be noted that the costs associated with a continuous fermentation setup consumes about half of total plant capital.

Table 7.2a. Capital cost broken down by equipment type

Equipment Type	Capital Cost (USD)
Pumps	\$4,574,240
Conveyors	\$736,300
Heat Exchangers	\$2,186,158
Columns	\$6,471,830
Tanks	\$177,801,800
Filters	\$30,118,037
Fermentation	\$204,716,740
Milling	\$359,133
Total Capital Cost:	\$426,964,238
CEPCI Adjusted:	\$645,197,721
Lang Factor (3.63)	
Adjusted/ FCI:	\$2,342,067,726

The total capital cost for plant equipment was adjusted using the chemical engineering plant cost index (CEPCI), and Equation 7.2a to find equivalent equipment pricing in today's dollars. A value of 800 was used to evaluate 2024 pricing (*Chemical Engineering Plant Cost Index*). Once adjusted for the CEPCI, the total capital cost was adjusted using the lang factor for a solids-fluids processing plant, 3.63. This factor scales the plant's capital costs, accounting for piping, permitting, land, as well as offices, roads, and facilities. A total, scaled, fixed capital investment (FCI) for the plant of about \$2,342,068,000 is found in Table 7.2.a.

$$\text{Current price} = (\text{given dated price}) * \left(\frac{\text{current CEPCI}}{\text{dated CEPCI}} \right)$$

Equation 7.2a. Conversion from old price data to new price data using CEPCI

7.3 Feed Costs and Product Revenue

Table 7.3a depicts yearly costs and revenue associated with the process. Corn stover pricing was determined based on the common, current market price of around \$600/MT, (translating to \$0.06/kg). Purchased water per year, which accounts for the makeup water needed after recycling all of the water waste streams in the process, was priced as process water. The initial amount of water needed at Year -1 and 0, was taken into account in the initial capital cost calculation. The acid and base were priced based on current industrial market estimates.

The main driver of revenue, as seen in Table 7.3a, is the CaHPO₄ animal feed supplement product created in the acid pretreatment block. The price for this product was based on the advertised price for a 22 wt.% CaHPO₄ animal feed supplement, which is \$0.64/kg. Because of assumed impurities in this project's product, including corn stover, leftover cell waste, and trace minerals, the team decided to cut the price to about 75% of this listed price. This was an arbitrary discount price that attempts to take these impurities into account. As discussed later in this report, this price needs to be verified and optimized through further research to make the following economic analysis more realistic. Butanol product was priced using the current standard market price of \$1.10/kg.

Table 7.3a Yearly Cash Flow: Feedstock & Product Costs and Revenues

Feedstock Type	Price/kg (USD)	Consumption (kg/yr)	Cost (USD/yr)
Corn Stover	\$0.06	1,300,000,000	\$71,500,000
Purchased Water	\$0.0003	1,720,800,000	\$536,890
<i>Clostridium Acetobutylicum ATCC 824</i>	--	--	**1,000,000
75% Phosphoric Acid	\$1.10	590,400,000	\$649,440,000
Anhydrous Ca(OH) ₂	\$0.24	331,200,000	\$79,488,000
Total Cost:			\$800,964,890
Product Type	Price/kg (USD)	Production (kg/yr)	Revenue (USD/yr)
Butanol	\$1.10	57,600,000	\$63,360,000
CaHPO ₄ Animal Feed Supplement	\$0.50	2,944,800,000	\$1,472,400,000
Total Revenue:			\$1,535,760,000
Total Profit:			\$734,795,110

** This is a needed feedstock, but is a fixed capital only bought in year 0; it is not included in the total cost/year

7.4 Total Operating Costs

Table 7.4a depicts all of the total operating costs for the butanol plant. Three main utility types were used in plant operations and contributed to operating costs: electricity, steam, and cooling water.

Table 7.4a Total Operating Costs with reduction from ethanol and acetone burning

Utility Type	Energy Consumption (kW)	Consumption (kg/yr)	Operating Cost (USD/yr)
Electricity	3,015	-	\$2,873,100
Steam	-	4,904,855,010	\$89,332,200
Cooling Water	-	68,545,595,314	\$3,535,400
Total Operating Cost Per Year:			\$95,740,700
Utility Type	Energy Consumption (kW)	Production (kg/yr)	Operating Cost Reduction (USD/yr)
Burning Ethanol and Acetone	-	14,400,000	\$5,796,500
ACTUAL Utility Cost per Year:			\$89,944,200

Steam and cooling water usage and associated costs were primarily found using the Process Economics Analyzer in AspenPlus. Generic steam price was based on January 2019 value, and found to be about \$0.02 dollars/kg (*Industrial Steam Cost: Industrial Utilities*). Generic cooling water price was based on January 2019 values, and found to be about 0.0048 cents/kg of water (*Cooling water cost: Industrial utilities*). Generic process water price was also based on January 2019 values, found to be about 0.031 cents/kg of water (*Process water cost: Industrial Utilities*). Electricity consumption and costs were found via AspenPlus for more

complex designs. For more simple designs like some pumps, the Plant Design and Economics for Chemical Engineers 5th edition was utilized, along with equation 7.1a (Peters et al., 2003).

Labor was assumed to be another operating cost the plant would allocate money towards each year. To estimate labor requirements, a few assumptions were made using data from Peters et al. (2003), Towler & Sinnott (2012), and the Iowa BLS (*Chemical plant and System Operators*). From Peters et al. (2003), the plant is classified as a highly automated, large equipment facility that produces about 172 tons of product per day, using the average number of employees per ton of product (3) for a solids-fluids processing plant, operating at 300 days per year to get an operating labor requirement of 51,597 employee hours per year. Using Iowan BLS for chemical plant manufacturing, the hourly operating employee wage is \$28.20 per hour. Supervisory labor is about 1.2 times the yearly operating labor cost (Peters et al., 2003). Benefits for employees were found via Towler & Sinnott (2012), using a value of 1.5 times the overall labor cost per year. Ultimately, labor required to operate the plant came out to \$4,801,616 per year.

There are additional nonmaterial costs based on the fixed capital investment that are considered yearly costs for the plant, including local property taxes, legal fees, and insurance. According to Peters et al., (2003), local property taxes for a plant situated in a sparsely populated area is about 2% of the plant’s FCI, while legal fees and insurance are about 1% of FCI. These values can be seen in Table 7.4b.

Table 7.4b Nonmaterial Operating Costs

Nonmaterial Operating Costs	Cost (\$/yr)
Labor	\$4,801,600
Insurance	\$23,419,700
Legal Fees	\$23,419,700
Local Property Tax	\$46,841,400

7.5 Cash Flow and DCF Analysis

7.5.1 Cash Flow Calculation

To determine before-tax cash flow, the yearly costs of the plant were subtracted from the expected yearly revenue. Costs included capital and operating costs, and revenue was generated from the sale of products. The result from the subtraction of these numbers was the profit, or cash flow, of the plant for the given year.

After-tax cash flow took yearly cash flow and subtracted taxes due for the given year. An important part of the calculation of taxes for this plant is depreciation. A 9.5 straight-line depreciation is a conservative annual depreciation value suggested by Peters et al., (2003). Peters et al., (2003) calculates depreciation, d , in Equation 7.5.1a where V is the value of the original investment or FCI, and n is the length of the straight-line receiving period (9.5).

$$d = \frac{V}{n}$$

Equation 7.5.1a Depreciation equation

Thus for 9.5 years, the depreciation was subtracted from the profit cash flow and the resulting value is what taxes were based upon. After 9.5 years federal and state taxes were based on the unadjusted profit of the plant. A federal tax rate of 21% was used, while Iowa state taxes are 5.5% (Watson, 2023; *State corporate income tax rates and brackets for 2024*). Both tax rates were pulled from current, 2024 values.

The before and after tax cash flows can be seen in Figure 7.5.1a. The cumulative cash flow over time can be seen in Figure 7.5.1b. It can be seen that the plant breaks even at around year five when the cumulative cash reaches a value of zero.

Working capital was calculated to be 10% of the plant's FCI, as per Peters et al., (2003). Working capital allowance was split evenly between years -1 and 0 to account for the plant beginning operation at half capacity in year -1.

Construction for the plant was based on an 18 month schedule, where beginning from year -2 to -0.5 the plant did not operate. According to Peters et al., (2003), costs associated with construction are about 8% of the plant's FCI per year. From year -0.5 to year 0, the plant ran at half capacity, reducing materials consumed, saleable product, and utilities by half their yearly amount.

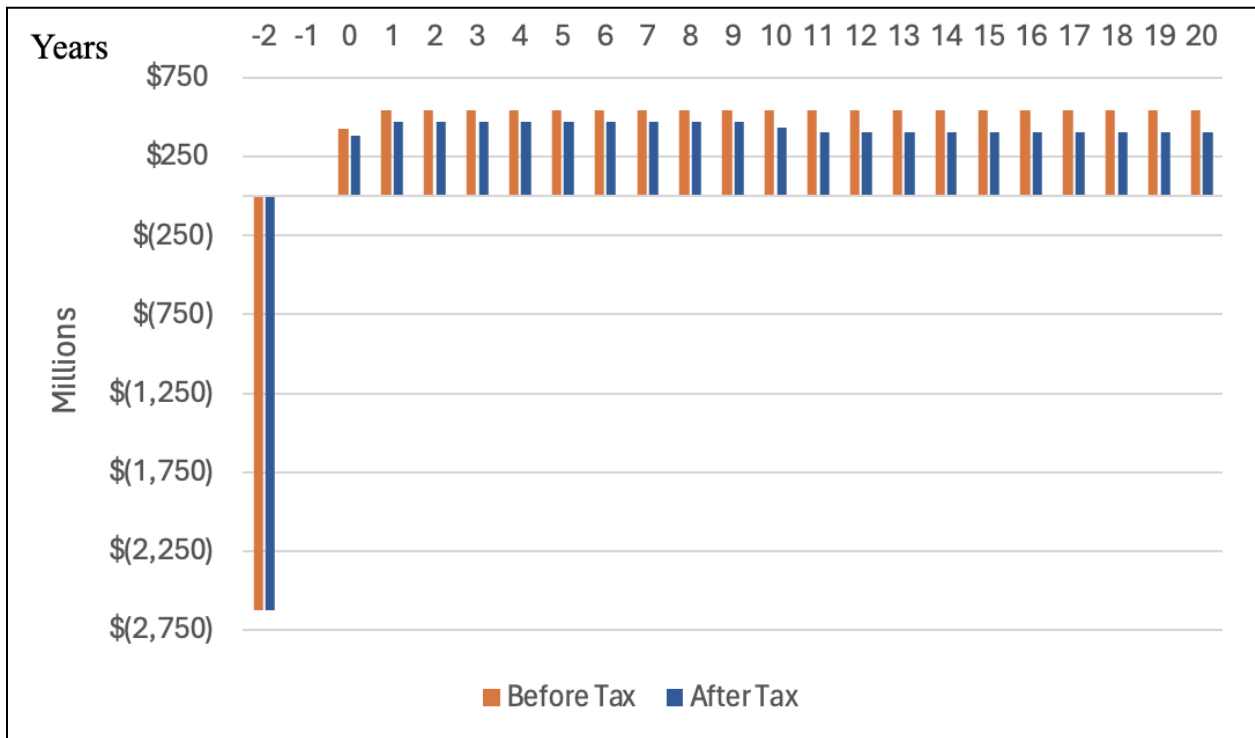


Figure 7.5.1a. The before and after tax cash flows from year -2 to year 20

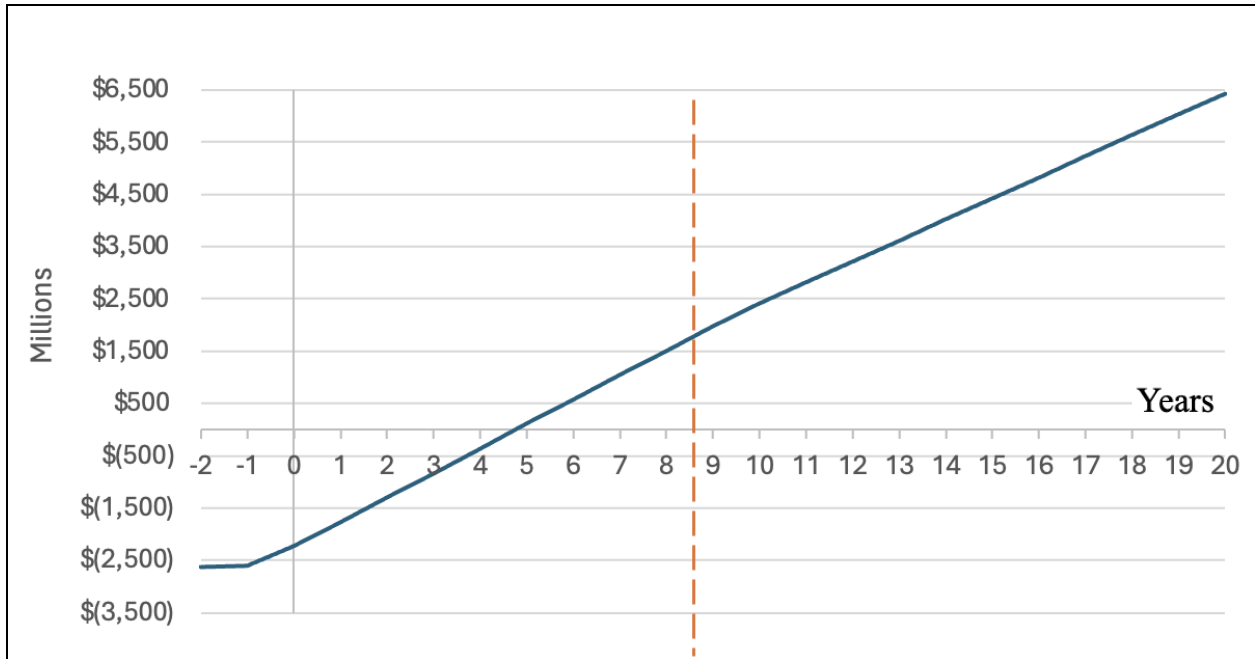


Figure 7.5.1b. The cumulative cash flow over 20 years

7.5.2 DCF Analysis and IRR Calculation

Once the after-tax cash flow for 20 years of operation was determined, a discounted cash flow (DCF) analysis was performed. This was done by taking the after tax cash flow for each year and multiplying it by the discount rate. The discount rate for each year was determined using equation 7.4.3a. The interest rate used in this calculation was the prime rate, which as of March 2024 is 8.5% (*Board of governors of the Federal Reserve System*). The prime rate was selected given that this project would likely be built by an established company that would qualify for the prime rate.

$$Discounted\ Cash\ Flow = \frac{(Cash\ Flow)}{(1 + interest\ rate)^{year}}$$

Equation 7.4.2a Discounted Cash Flow Equation

The product of the discounted cash flow and the discount rate are considered the discounted cash flow. The summation of these discounted cash flows is the net present value

(NPV). For our analysis the NPV was determined to be \$1,526,348,116. This positive value indicates that this investment should be profitable in the long run (*A refresher on Net present value*).

The internal rate of return (IRR) was also calculated in this analysis. The internal rate of return is the interest rate in the discounted cash flow equation that makes the net present value zero. This was done using the Excel IRR() function, which returned a value of 13.9%. It makes sense that this IRR value is greater than the prime rate given the positive NPV. Due to current economic conditions, the prime rate is much higher than it has been in past years. If the prime rate were to drop, or if this project could qualify for a lower interest rate, this could make the plant more attractive to investors.

8. Safety, Health, Environment, and Social

8.1 Introduction

As part of overall plant design, it is critical to consider and evaluate the potential safety risks associated with the butanol production process. The stakes are high, not only in terms of potential human and environmental harm but also in terms of financial and reputational consequences. Thus, thorough consideration of process safety concerns is indispensable in the planning, design, and operation phases of any facility. To highlight these concerns, a chemical reactivity matrix will be constructed including all reactants and products used site wide. Then, a safety analysis of the facility will be divided into process blocks, and a Maximum Credible Event (MCE) will be determined. Additionally, a source model for each MCE will be developed, and necessary process controls will be recommended if applicable.






8.2 Chemical Hazard Table

To construct the chemical hazard table (Table 8.2a), two SDS documents were cross referenced, and the more conservative measurement across the two was included on the table. Hazard statements included in either SDS document were added to the table; these SDS documents can be accessed through the links in Appendix 8.12.2. The chemical hazard table highlights the hazards associated with all of our hydrocarbon products. Precautions should be taken to mitigate the probability of an explosion or ignition, especially in areas of the process where the potential for vapor phase hydrocarbons exists. Also notable is that the team's facility would be governed by OSHA PSM guidelines since over 10,000 lbs of flammable materials exists on site at all times, requiring our facility to comply with OSHA 1910.119. Many of the chemicals present are skin and eye irritants, so eyewash stations and emergency showers should be readily available in all employee-occupied spaces. The chemical hazard table does not

illustrate some other process hazards such as temperature, pressure, and mechanical hazards.

These will be discussed in the individual process block sections.

Table 8.2a Chemical Hazards

Chemical Hazard Table For Bio-Butanol Production Facility					
Chemical	Acetone	Calcium Hydroxide	Ethanol	Butanol	Phosphoric Acid
Location	Fermentation Separations	Storage Pretreatment	Fermentation Separations	Storage Fermentation Separations	Storage Pretreatment
CAS Number	67-64-1	1305-62-0	64-17-5	71-36-3	7664-38-2
Signal Word	Danger		Danger		Danger
GHG Pictograms					
Hazard Codes	H225 H319 H336	H315 H318 H335 H402	H225 H319	H226 H302 H315 H318 H335 H336	H290 H302 H314 H318
Hazard Statements	Highly flammable liquid and vapor Causes serious eye irritation May cause drowsiness or dizziness	Causes skin irritation Causes serious eye damage May cause respiratory irritation Harmful to aquatic life	Highly flammable liquid and vapor Causes serious eye irritation	Flammable liquid and vapor Harmful if swallowed Causes skin irritation Causes serious eye damage May cause respiratory irritation May cause drowsiness or dizziness	May be corrosive to metals Harmful if swallowed Causes severe skin burns and eye damage
Molecular Weight (g/mol)	58.08	74.09	46.07	74.12	98
Boiling Point (°C)	56	2,850	78	116	158
Flash Point (°C)	-17	N/A	13	35	N/A
Auto Ignition Temp (°C)	465	> 400	363	340	N/A
OSHA PSM TQ (lbs)	10,000	N/A	10,000	10,000	N/A
LFL (vol%)	2.0	N/A	3.1	1.4	N/A
UFL (vol%)	13.0	N/A	27.7	11.2	N/A

8.3 Chemical Reactivity Matrix

To construct the chemical reactivity matrix, two matrices were collated. One from CAMEO Chemicals, and the other from AICHE CRW 4. Individual matrices can be found in Appendix 8.12.1. Based on the results of the matrix, several mixtures of process chemicals generate heat. While these mixtures do occur in regular operation of the facility, they do so under very dilute conditions. The magnitude of heat generated from their mixture as predicted by ASPEN simulation is not hazardous, and in practice can be used to offset heat exchanger duties.

The explosive nature of the hydrocarbon mixtures is also seen in the matrix and as mentioned previously is a prominent hazard within the process. Implementing engineering and administrative controls to mitigate the danger will be necessary. Engineering controls can include

both proper ventilation systems as well as hydrocarbon vapor detection systems. Administrative training on the dangers of the products and emergency procedures should also be established.

Finally some of the reactants to our process pose significant health hazards. Since substituting them for a less-hazardous option is not a viable option, minimizing employee exposure to these chemicals is critical for site safety. Using enclosed material handling practices for our calcium hydroxide is a necessary precaution. Likewise, wearing appropriate PPE when in the vicinity of phosphoric acid processing is an important last line of defense for safety.

NFPA Diamond			Chemical Reactivity Matrix For Bio-Butanol Production Facility						
Health	Flamability	Instability	Species	Acetone	Calcium Hydroxide	Ethanol	Butanol	Phosphoric Acid	Water
1	3	0	Acetone						
3	0	0	Calcium Hydroxide						
2	3	0	Ethanol	Explosive Unstable when heated					
2	3	0	Butanol	Explosive Unstable when heated					
3	0	0	Phosphoric Acid		Generates heat				
0	0	0	Water		Generates heat			Corrosive Generates heat	

Figure 8.3a Chemical Reactivity Matrix

8.4 Storage Safety Analysis

Storage for the butanol production facility represents a significant hazard. Large quantities of flammable hydrocarbons as well as highly combustible organic material are present. Large grain silos pose significant combustible dust hazards due to the accumulation of fine grain particles in the air, creating a potentially explosive atmosphere. When dispersed and ignited, these dust particles can result in detonation. Research conducted by the North Carolina Department of Labor (Berry et al. 2012) found that the lower explosive limit of milled corn was 55 g/m³. With this in mind, the team has determined that storing unmilled stover is preferential to the safety risks and economic costs associated with storing milled stover. As implementing the required equipment to operate below the 55 g/m³ threshold would be costly to implement and

maintain. Unmilled stover is not without risk though. Storing dry, combustible organic material in the quantities the plant requires some additional safeguards. The storage bins where the dry stover is stored should all be fitted with fire monitoring systems such that a fire within the bin could be detected rapidly after onset. In addition, a water deluge system to put out any fires should also be installed and be remotely operable to minimize risk to plant personnel.

Another significant storage hazard are the bulk product storage tanks. While the team intends for the plant to constantly offload butanol product to tanker trucks, there will still be some accumulation in storage before this can occur. The team estimates a 334,050 gallon tank will be required for this purpose. In order to quantify the hazards associated with storing this product, an ALOHA model was created by the team. In order to generate results, several conservative assumptions were made, which are specified in Appendix 8.12.3. The first model the group made was for a liquid release generating a vapor cloud. The results of this model can be seen in Figure 8.4a. The model illustrates a cloud that does not exceed the IDLH or LEL thresholds, likely owing to the low volatility of butanol relative to other small hydrocarbons.

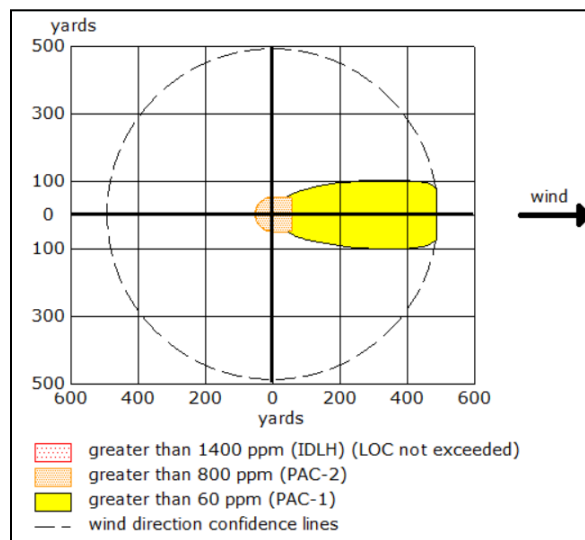


Figure 8.4a Storage Toxic Cloud

The next model created was for a pool fire, resulting from the same magnitude of leak, but this time burning. While this is unlikely, with the liquid being stored well below its flash point, it is important to consider. The pool fire model (Figure 8.4b) shows a potentially lethal burn hazard in an approximately 30 meter radius around the tank, and second degree burns occurring up to 50 meters away.

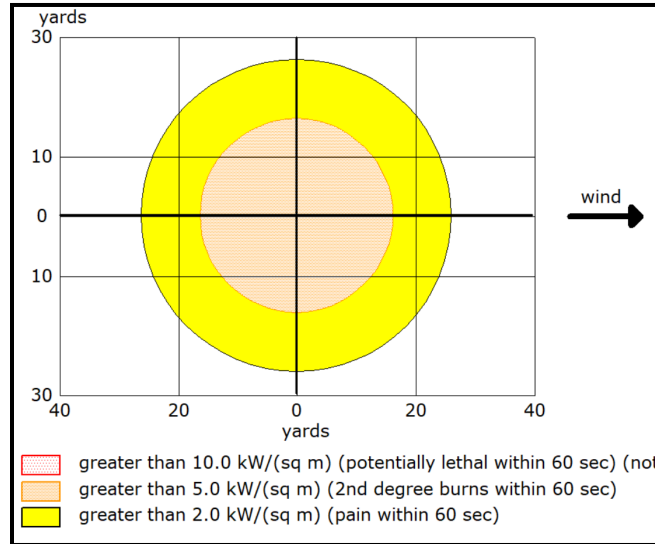


Figure 8.4b Storage Pool Fire

Finally the team modeled a boiling liquid expanding vapor explosion (BLEVE) from this storage tank. However, it was determined to be very highly unlikely, as the butanol is stored at ambient temperature and atmospheric pressure, with no direct connections to potential additional heat sources. While the results of this model (Figure 8.4c) depict a devastating explosion, the probability of conditions existing to enable such an exposition is low enough to accept the risk associated with a BLEVE.

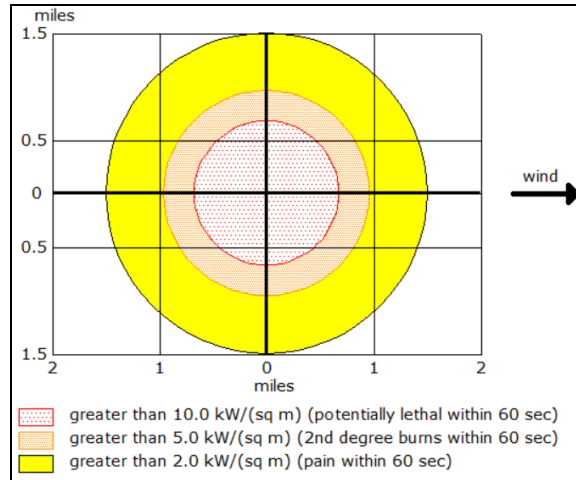


Figure 8.4c Storage Tank BLEVE

Considering these models, the team would divide storage into multiple tanks to reduce the quantity of flammable materials stored together if the process was to be developed further. Additionally, inventory should be tightly controlled to minimize the quantity of butanol stored on site at any given time, and construction of a dike surrounding the storage tank should occur.

8.5 Milling Safety Analysis

The hammer mills used in our process represent a significant mechanical hazard. If employees were to unexpectedly enter the machines while operational or the mills were to be turned on while maintenance activities are happening, the potential for employee injury is high. In order to mitigate the potential for injury, proper lockout-tagout procedures for large equipment like the mills should be generated and followed rigorously. Furthermore, implementing engineering controls to prevent accidental entry to the machine also decreases the potential for injury.

The dry milling process the team has chosen has the consequence of generating a significant amount of potentially combustible dust. To mitigate this hazard, several layers of protection will be adopted in the milling process. Firstly, regular maintenance and cleaning of

hammer mills are essential to minimize dust accumulation. Additionally, utilizing proper ventilation systems aids in controlling dust dispersion and maintaining safe air quality within the milling area and installation of enclosed conveyors prevents aerosolization. Finally, training employees on dust control measures and emergency procedures plays a crucial role in preventing accidents and ensuring a safe working environment within grain handling facilities.

8.6 Acid Pretreatment Safety Analysis

The pretreatment process incorporates several hazards. Firstly, there are the chemical hazards associated with calcium hydroxide and phosphoric acid which were highlighted in Table 8.2a. It is important to note here that phosphoric acid solutions are highly corrosive to metal, and choosing equipment that can resist corrosion is necessary wherever concentrated phosphoric acid is present. For this reason, our bulk acid and base tanks are constructed of 316 stainless steel which should remain durable for the life of the plant.

The pretreatment process also involves solids handling for the calcium hydroxide. It is important to keep the solid base dry and the system enclosed. As creating concentrated solutions of calcium hydroxide could damage process equipment and any accidental inhalation is highly dangerous to employees. To accomplish this, a conveyor system will be used to transport calcium hydroxide to the neutralization reactor, and appropriate PPE including self contained breathing apparatuses (SCBA) will be available in the event of an emergency in all process areas containing these chemicals.

Furthermore, the pretreatment process involves high temperatures (103°C), and above ambient pressures. These conditions necessitate robust piping around process equipment. Stainless steel will likely be used for this as well, and the piping will also require insulation to

protect from accidental burns. This part of the process also represents a significant environmental hazard which will be discussed in the environmental section.

8.7 Fermentation Safety Analysis

The fermentation part of the process is largely less hazardous than other blocks. While physical hazards and the threat to employees is low relative to other unit operations, it is still worth considering the biological impact this process might have. *Clostridium acetobutylicum* are far less dangerous than the other *Clostridium* strains that cause gangrene and botulism. They are not known to produce any toxins or cause any virulence in mammals (EPA 1997). However, it is important that our fermenters grow this passive strain of *Clostridium* and not a virulent strain. To ensure this, a holistic sterilization and inoculation procedure of process fermenters will be developed.

Another hazard associated with the fermentation process is the size of the primary fermenters, with a capacity of 10,000 m³ each, inspecting the tanks for damage can be a dangerous task. Ensuring that any employee inspecting the roof of the tank or climbing up the tank in any capacity should undergo proper fall prevention training and wear a fall protection harness when outside of designated areas. Lastly, the ABE fermentation process generates carbon dioxide, which could suffocate an employee if it accumulates in a confined space. To prevent this, carbon dioxide level monitors can be placed around the primary fermenters to monitor for any increase in carbon dioxide concentration.

8.8 Separations Safety Analysis

The separation area of the facility has a significant number of hazards, both in terms of process equipment and in hydrocarbon presence. The first of which involves the pervaporation steps within the separation processes. These must be conducted using near-vacuum conditions to

drive flux through a membrane. These membranes operate with a vacuum around 280 Pa, so vacuum implosion is a possibility. To mitigate this, careful reactor design should go into the construction of the housings for this step to ensure they are rated to withstand repeated vacuum cycles without fatigue.

The next hazard in the process are the distillation columns that purify our products and separate out water. Many of the substances being distilled in our process are flammable or combustible. During distillation, these substances may vaporize and form an explosive atmosphere if not properly controlled. Any ignition source, such as sparks from electrical equipment or hot surfaces, can lead to fires or explosions. Adequate ventilation, explosion-proof equipment, and strict adherence to safety protocols are essential to mitigate these risks. It is also critical that the temperature regulation to the column condenser remains operational to stop the column from overheating. Finally, keeping the hydrocarbon vapors within the process equipment is not only important for physical safety, but also environmental considerations.

The products of the separation process and the process as a whole include several flammable and volatile products. Both the butanol stream and acetone/ethanol streams were modeled in ALOHA to quantify the potential impacts of an incident. To generate these results, assumptions outlined in Appendix 8.12.3 were made. The first model (Figure 8.8a) depicts the toxicity of a full release of the acetone and ethanol product stream.

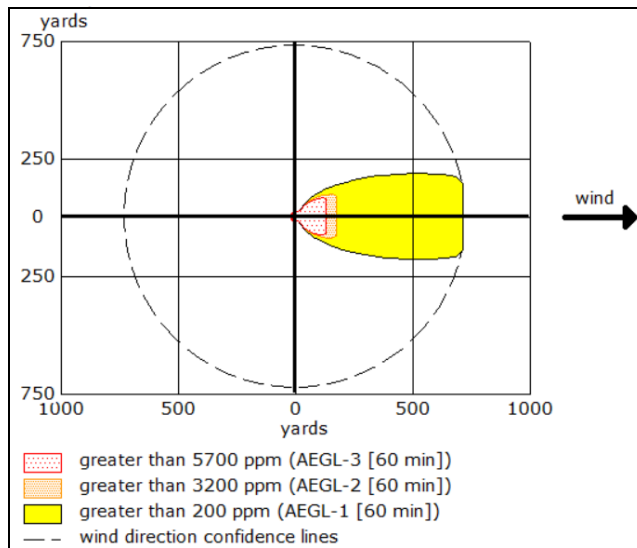


Figure 8.8a Toxic Cloud from Acetone & Ethanol Product Stream

This model depicts a concentration of 5700 ppm up to around 100 yards downwind of the release, which would constitute an exposure that is life-threatening or deadly. The model predicts noticeable and uncomfortable exposure beyond 600 yards away as well.

The next model analyzed this same source for flammability. As seen in Figure 8.8b, concentrations exceeding the lower explosive limit were present up to 60 yards away from the release. This magnitude of release has the potential to find an ignition source well within the LEL envelope. The modeling of the overpressure from a resulting explosion is seen in Figure 8.8c.

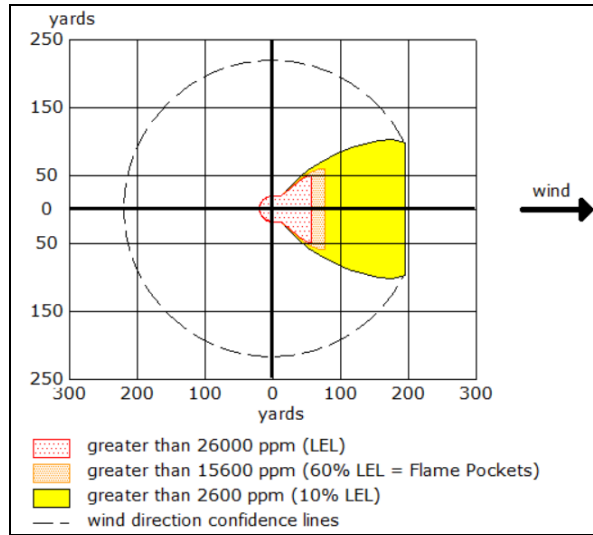


Figure 8.8b Flammable Cloud from Acetone & Ethanol Product Stream

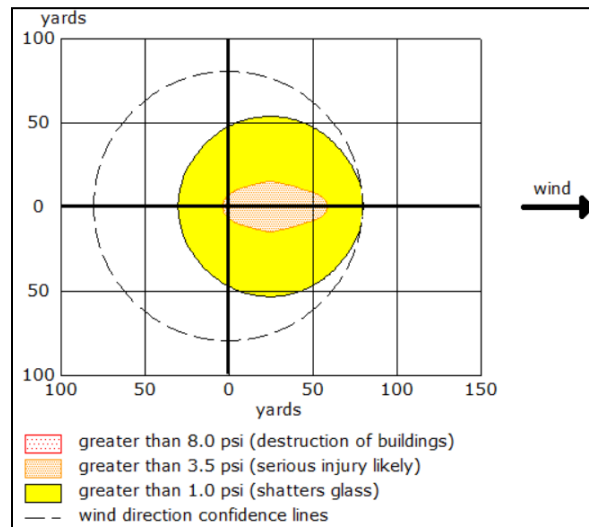


Figure 8.8c Overpressure map from Acetone & Ethanol Product Stream VCE

Based on the model, serious injury is likely over 50 yards away, and process equipment is likely to be damaged in around a 50 yard radius from the initial explosion. The same models were generated for the butanol product stream following similar assumptions. The toxic vapor cloud for the butanol product stream can be seen in Figure 8.8d. The model highlights the potential severity of a release of all of our product, with PAC-1 exposure limits being exceeded

over a mile downwind, this type of release represents a significant hazard to the plant and surrounding community.

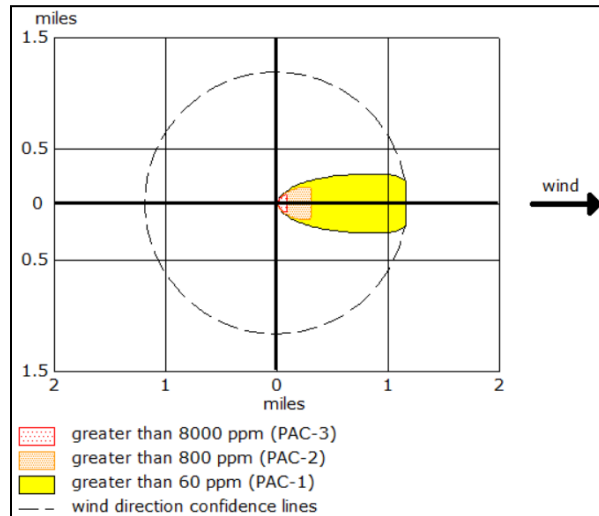


Figure 8.8d Toxic Cloud from Butanol Product Stream

Analyzing this same release for flammability gives the model in Figure 8.8e. This figure shows a concentration of butanol above the LFL over 100 yards away from the initial source of the release. With this level of dispersion, a resulting explosion is highly likely. The overpressure wave resulting from this is shown in Figure 8.8f.

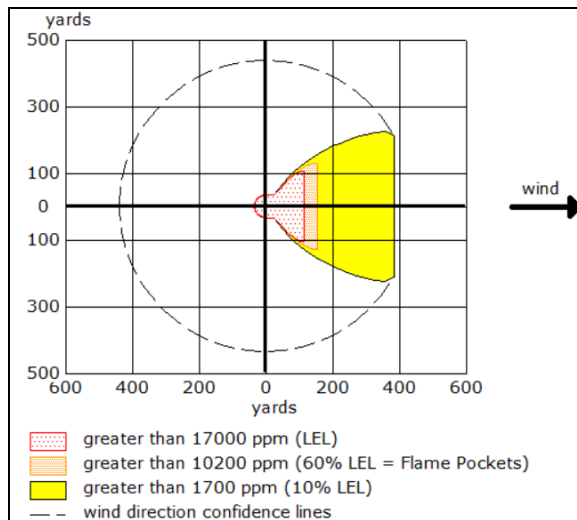


Figure 8.8e Flammable Cloud from Butanol Product Stream

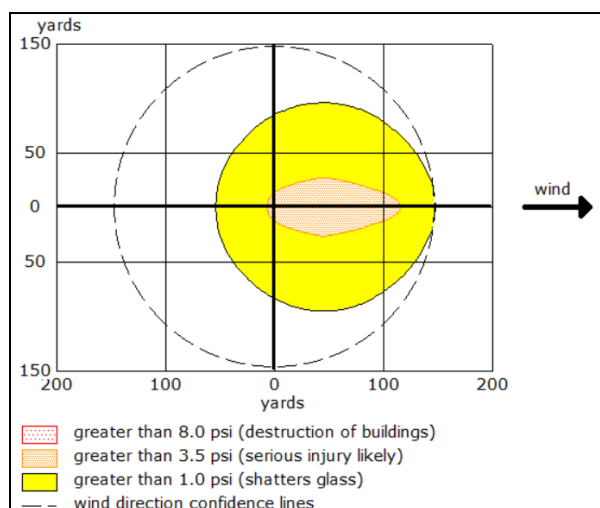


Figure 8.8f Overpressure map from Butanol Product Stream VCE

This figure indicates serious injury occurring over 100 yards downwind of the initial explosion and damage to process equipment and buildings over 100 yards in all directions. This release represents the most significant hazard within the process. With potential toxic effects over 1 mile away, and a high likelihood of a fire or explosion following this release. Great consideration must be given to ensure the operation of the separation process and the hydrocarbon product streams. It is best to overbuild process piping in this portion of the plant as well as install blast proof shelters and control rooms around the separation process.

8.9 Safety Conclusion

The biobutanol production process is not without its risks. Flammable products, high temperatures, pressures, and mechanical hazards are all present within the facility. However, relative to traditional fuel production, the process is far more manageable and the potential impacts to the surrounding environment and community are much less. Overall, thorough examination of safety considerations at each stage of the butanol production process and utilization of practical measures can mitigate risks effectively. A proactive approach to process safety is essential for ensuring the well-being of employees, protecting the environment, and maintaining the integrity of the facility. By considering the dangers inherent to the process, an inherently safer design can be developed.

8.10 Environment

The environment in which this plant operates is primarily rural, with significant land dedicated to agriculture. There are also large waterways and groundwater that play an important role in both the local ecosystems and recreational use.

The impacts to health and safety discussed in the previous section can be extrapolated to impact on the environment and wildlife around the butanol plant. As such, if any of the chemicals discussed as part of the process were released into the environment it would be expected that damage to the environment would occur. Ecosystems and wildlife would be affected by the toxicity and other health hazards associated with these chemicals. It is expected that these impacts would be sustained in the environment until proper remediation efforts are taken by the company.

Barring any accidental releases of hazardous chemicals into the environment, it is expected that the normal, daily operation of our butanol plant would have minimal impact on the

environment. However, a loss of containment of the phosphoric acid or calcium phosphate bears significant environmental consequences, as both compounds bear mild acute and major chronic toxicity concerns to aquatic organisms, an especially alarming impact considering the local ecosystem (DCCEEW 2022). Installing dikes around our acid and base storage locations would help mitigate the environmental dangers they pose and contain any accidental spills. All local and federal waste disposal laws will be followed to prevent damage from the waste streams coming out of fermentation and the separation process. Water usage is kept to a minimum through the use of a recycle stream for our main water requirement. Our plant is inherently more “green” than competing fossil fuel facilities due to the conversion of an agricultural waste product into a sustainable fuel additive. However, concerns about energy demands and commodity transportation, and the subsequent emissions created as a result, remain when evaluating the environmental impact of our facility. The electricity and steam requirements for this process may contribute to greenhouse gas emissions, however, if these can be sourced from green producers of energy that would be ideal. Future investment into renewable energy should be evaluated. There are also carbon dioxide emissions from the anaerobic ABE fermentation, which is being vented to the atmosphere. Carbon capture technology should be evaluated to address this. The transportation of feedstock and product materials is expected to contribute to greenhouse gas emissions as well and attempts should be made to make these transportation methods as “green” as possible.

Waste disposal and management is a key environmental consideration in the design and operation of the facility. With respect to Iowa state law concerning the disposal of industrial waste, governed specifically by Iowa Code 567.109 (Iowa Legislature 2008), which covers specifications of the contents of the waste, the weight and volume of the waste generated and

other relevant characteristics of the waste necessary to ensure proper disposal will have to be evaluated at the scope of our plant. Special waste permitting in compliance with state law will be required for our operation due to 1) the production of biologically active waste material and 2) the disposal of large amounts of liquid waste that contain residual organic solvents. Covering the cost of waste disposal varies based on the particular type of waste. Specifications in law can be found in Iowa Administrative Code r.567-149.4, which details costs associated with the transportation of and disposal or destruction of hazardous process waste. Pricing of waste disposal is also offered by private ventures, which also cover management of waste type and include compliance in their services. Alternatively, the plant could divert part of the waste acetone and ethanol stream to incinerate dried biomass, covering the combined cost of disposal of liquid, solid and biologically active waste otherwise applicable under Iowa law. Further discussion of waste disposal measures is left for the Conclusions and Recommendations portion of this paper.

8.11 Social

The construction of this plant would affect the surrounding community in areas outside of safety and the environment. The plant will bring jobs into the community during both the construction phase and the operation phase, which is expected to benefit the local economy.

The geographic size and expected operation noise of this plant will impact the surrounding community, but the rural distribution of the population will help mitigate these effects. Additionally, with proper community outreach and by building positive relationships with our neighbors, the team does not expect this to be an issue in the long term.

Of particular note is the economic impact of the sale of our animal feed supplement. With Iowa farms and ranches raising the most hogs and laying chickens of any state, as well as being

responsible for fifteen percent of the nation's red meat production (Thessen et al. 2023), the newly available feed supplement that our facility offers will no doubt be a welcome addition to the local markets. With feed and supplements comprising up to seventy percent of the costs of raising livestock to marketable quality (Strauch & Stockton 2013), the ability to supply nutritional supplementation at competitive prices is a key positive for our facility.

8.12 Safety Appendix

8.12.1 Chemical reactivity matrices

Y : Compatible N : Incompatible C : Caution SR : Self-Reactive * : Changed by user				ACETONE	CALCIUM HYDROXIDE	ETHANOL	N-BUTYL ALCOHOL	PHOSPHORIC ACID	WATER
NFPA Health Flammability Instability Special				Bio-Butanol Production Facility Compatibility Chart					
1	3	0							
				Y					
2	3	0		C	Y				
2	3	0		C	Y	Y			
3	0	0		Y	C	Y	Y		
				Y	C	Y	Y	C	

	WATER				
PHOSPHORIC ACID	Caution Corrosive Generates heat	PHOSPHORIC ACID			
CALCIUM HYDROXIDE	Caution Generates heat	Caution Generates heat	CALCIUM HYDROXIDE		
N-BUTYL ALCOHOL	Compatible	Compatible	Compatible	N-BUTYL ALCOHOL	
ETHANOL	Compatible	Compatible	Compatible	Compatible	ETHANOL
ACETONE	Compatible	Compatible	Compatible	Caution Explosive Unstable when heated	Caution Explosive Unstable when heated

8.12.2 Safety Data Sheet Sources

Sources	SAFETY DATA SHEET	SAFETY DATA SHEET	SAFETY DATA SHEET	SAFETY DATA SHEET	SAFETY DATA SHEET
	SAFETY DATA SHEET	SAFETY DATA SHEET	SAFETY DATA SHEET	SAFETY DATA SHEET	SAFETY DATA SHEET
Chemical	Acetone	Calcium Hydroxide	Ethanol	Butanol	Phosphoric Acid

8.12.3 ALOHA Assumptions

ALOHA Assumptions (**Storage**)

- Stability Class F
- Lowest Possible Wind Speed (2.3 mph)
- Open Country Environment
- 55 Fahrenheit Ambient Temperature
- 50% Relative Humidity
- Tank Height = $\frac{1}{3}$ Tank Diameter
- Chemicals Stored at ambient temperature
- Completely Full Tank (worst case)
- No vapor initially in tank (floating roof)

Evaporating Puddle & Pool Fire

- 2 inch diameter hole (20% largest estimated process pipe connected)
- Hole at bottom of tank
- Ground at ambient temperature

BLEVE

- 100% mass in fireball

ALOHA Assumptions (**Separations**)

- Stability Class F
- Lowest Possible Wind Speed (2.3 mph)
- Open Country Environment
- 55 Fahrenheit Ambient Temperature
- 50% Relative Humidity

Toxic Vapor Cloud (A&E Stream)

- 100 % Acetone output (ALOHA cannot model mixtures)
- Direct release of pipe contents
- One hour release duration

Overpressure Wave

- Congested area

Toxic Vapor Cloud (Butanol Stream)

- 100 % Butanol Output
- Direct release of pipe contents
- One hour release duration

Overpressure Wave

- Congested area

9. Final Recommended Design

9.1 Nomenclature

In this section of the report, specific streams and process equipment are identified using nomenclature that takes in account the block and equipment type. This nomenclature is as follows: [Block Abbreviation]-[Equipment Type Abbreviation][Equipment Number within Block]. The block abbreviations are defined in Table 9.a and the equipment type abbreviations are defined in Table 9.b.

Table 9.a Block Abbreviations

Block	Abbreviation
Storage	A
Milling	B
Acid Pretreatment	C
Fermentation	D
Separations	E

Table 9.b Equipment Abbreviations

Equipment Type	Abbreviation
Column	COL
Compressor	C
Decanter	D
Disk Filter	DF
Furnace	FR
Hammer Mill	HM
Heat Exchanger	HE

Pervaporator	PV
Pump	P
Reactor	R
Seed Fermenter	SF
Stream	S
Tank	T

9.2 Storage (Block A):

Table 9.2a Streams for Block A - Storage

Stream	A-S01	A-S02	A-S03	A-S04
Flow rate [kg/hr]	86,000	86,000	82,000	1,625,000
Dry Stover [wt. %]	93.8	93.8		
H2O [wt. %]	6.2	6.2	25	100
H3PO4 [wt. %]			75	

9.2.1 Feedstock storage

Dry corn stover required for one year of operation is stored in 47 storage bins A-T01 through A-T47 with a capacity of 28,000,000 kg each. For both phosphoric acid and anhydrous calcium hydroxide feedstocks, the plant will store one month's operating capacity. Phosphoric acid of 75 wt% is stored in one stainless steel floating roof tank holding about 49,200,000 kg of feed, A-T48. Anhydrous calcium hydroxide is stored in one steel cone roof tank holding around 27,600,000 kg of feed, A-T49.

9.2.2 Product Storage

All products will be stored in vessels sized at one operating month's capacity. The butanol product is stored in one steel floating roof tank holding about 49,200,000 kg, A-T71, while it awaits transport to the customers. The animal feed supplement product is stored in 21 storage bins, A-T50 through A-T70 with a capacity of 28,000,000 kg each.

9.3 Milling (Block B):

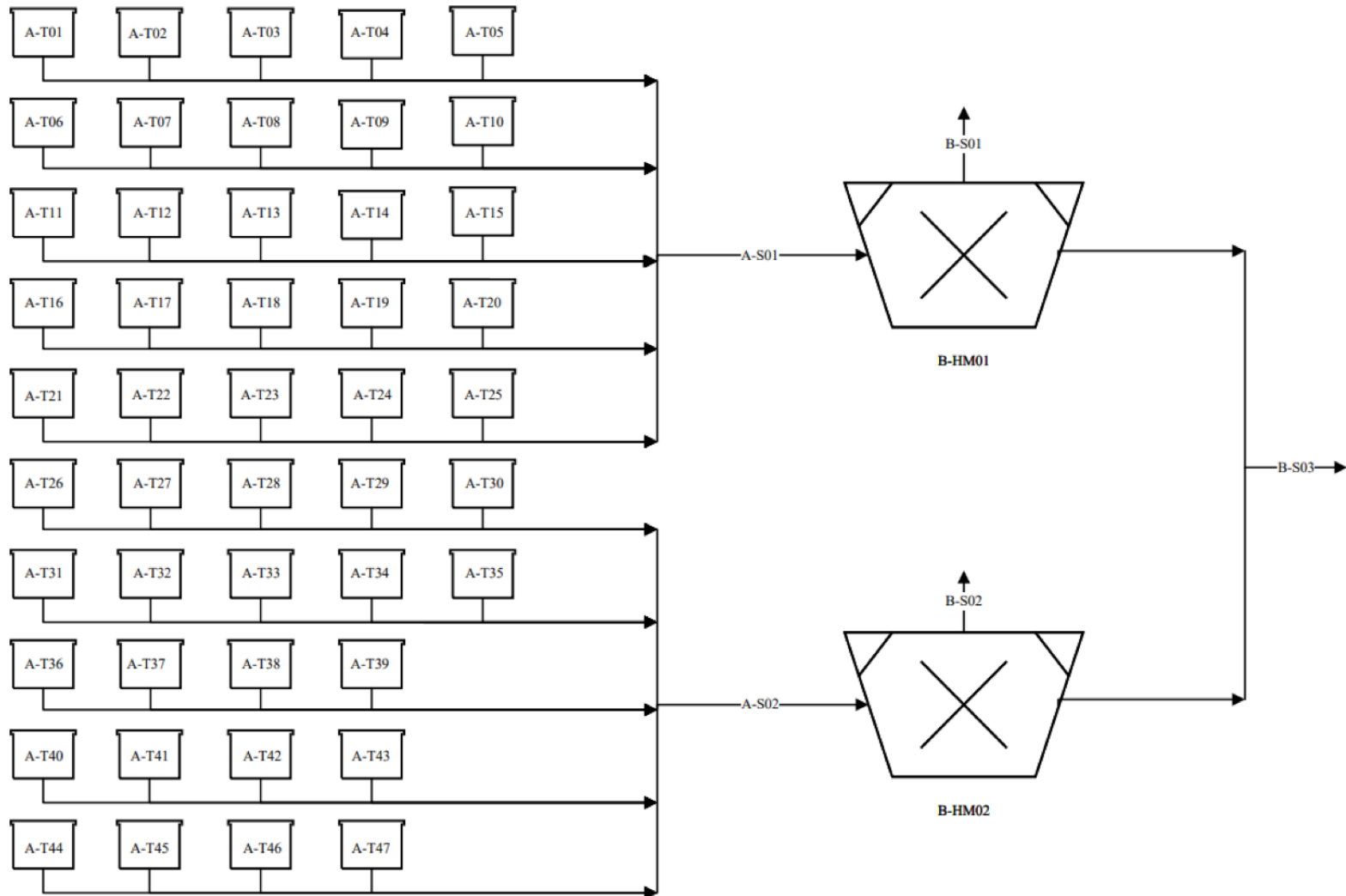


Figure 9.3a Milling Final Design

Table 9.3a Streams for Block B - Milling

Stream	B-S01	B-S02	B-S03
Flow rate [kg/hr]	4,500	4,500	172,000
Dry Stover [wt. %]	93.8	93.8	6.2
H2O [wt. %]	6.2	6.2	6.2

Conveyor belts are used to move corn stover from the storage containers in stream A-S01 and A-S02. Each stream enters a hammer mill, B-HM01 or B-HM02, where the size of the corn stover will be reduced to approximately 12.48mm chop size. Losses in this system due to the nature of hammer mill pumps are accounted for in streams B-S02 and B-S03. The milled stover will combine into stream B-S03 after the hammer mills where they are carried to the acid pretreatment block via another conveyer belt. All of these processes will take place at ambient temperature, i.e. 25°C.

9.4 Acid Pretreatment (Block C):

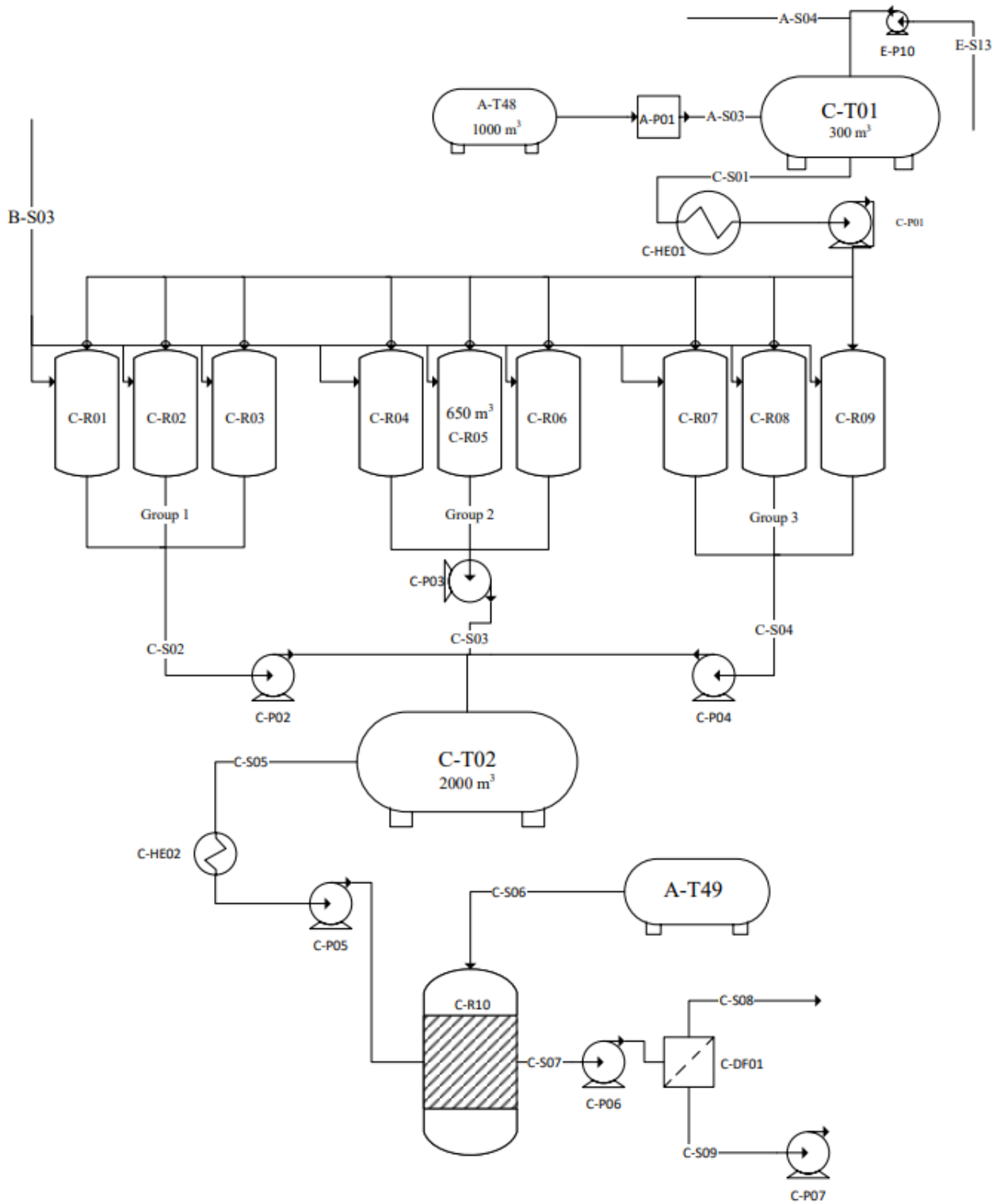


Figure 9.4a Acid Pretreatment Final Design

Table 9.4a Streams for Block C - Acid Pretreatment

Stream	C-S01	C-S02*	C-S03*	C-S04*	C-S05
Flow rate [kg/hr]	1,625,000	1,797,000	1,797,000	1,797,000	1,797,000
H2O [wt. %]	96.2	87.6	87.6	87.6	87.6
H3PO4 [wt. %]	3.8	3.4	3.4	3.4	3.4
Stover Waste [wt. %]		6.7	6.7	6.7	6.7
Glucose [wt. %]		2.3	2.3	2.3	2.3
Ca(OH)2 [wt. %]					
CaHPO4 [wt. %]					

* = follows specific reactor draining schedule, not a continuous flow

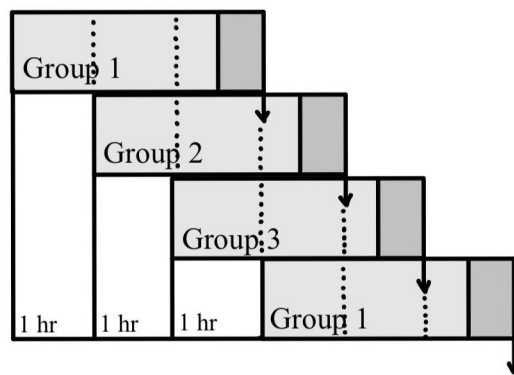
Table 9.4a (continued)

Stream	C-S06	C-S07	C-S08	C-S09
Flow rate [kg/hr]	46,000	1,843,000	409,000	1,434,000
H2O [wt. %]		85.0	50.0	97.0
H3PO4 [wt. %]				
Stover Waste [wt. %]		6.4	29.0	
Glucose [wt. %]		2.3		2.9
Ca(OH)2 [wt. %]	100.0			
CaHPO4 [wt. %]		4.5	21.0	0.1

From phosphoric acid storage tank A-T48, the 75 wt.% acid will be moved via pump A-P01 in stream A-S04 to dilution tank C-T01. This stream combines in C-T01 with the recycled water stream E-S13 and make-up water stream A-S04, which are moved with pumps E-P10 and A-P02, respectively. The resulting 3.76 wt.% dilute phosphoric acid stream C-S01 is pumped using pump C-P01 out of the dilution tank.

From the dilution tank, stream C-S01 of dilute phosphoric acid is heated in heat exchanger C-HE01 from 25°C to 103°C. Stream C-S01 is then split amongst a set of three reactor groups at a time. This stream is co-fed with stream B-S03, the milled corn stover. These

streams reach a temperature of 100°C after mixing inside the reactors to promote ideal reaction kinetics. There are three groups of three reactors, yielding a total of 9 reactors: C-R01 through C-R09. The three groups are C-R01 through C-R03, C-R04 through C-R06, and C-R07 through C-R09. These reactors follow the schedule presented in Figure 9.4a. The streams C-S02, C-S03, or C-S04 will be pumped out of the sets of reactors using pumps C-P02, C-P03, or C-P04, respectively. Streams C-S02, C-S03, and C-S04 combine into surge tank C-T02.



*The lighter gray region represents the reaction time for hydrolysis
and the darker gray region represents the draining and cleaning of the vessel.*

Figure 9.4b Reactor Scheduling

Stream C-S05, the combined slurry of glucose, waste stover, water, and acid, is pumped out of C-T02 using pump C-P05. C-S05 passes through heat exchanger C-HE02 to bring the temperature down from 100°C to 25°C. C-S05 is then passed into the neutralization reactor C-R10 where it is combined with stream C-S06. C-S06 is anhydrous calcium hydroxide delivered to C-R10 on a conveyor belt from A-T49. The final pH achieved in C-R10 is 4.41. Stream C-S07 exits reactor C-R10 where it is pumped by C-P06 through disk filter C-DF01 that separates corn stover filter cake into stream C-S08 and retains glucose and water solution in stream C-S09. C-S08 is pumped to storage tanks A-T50 through A-T70, a set of 21 storage

containers meant to hold this corn waste and CaHPO_4 rich stream. C-S09 is the feed to fermentation.

9.5 Fermentation (Block D)

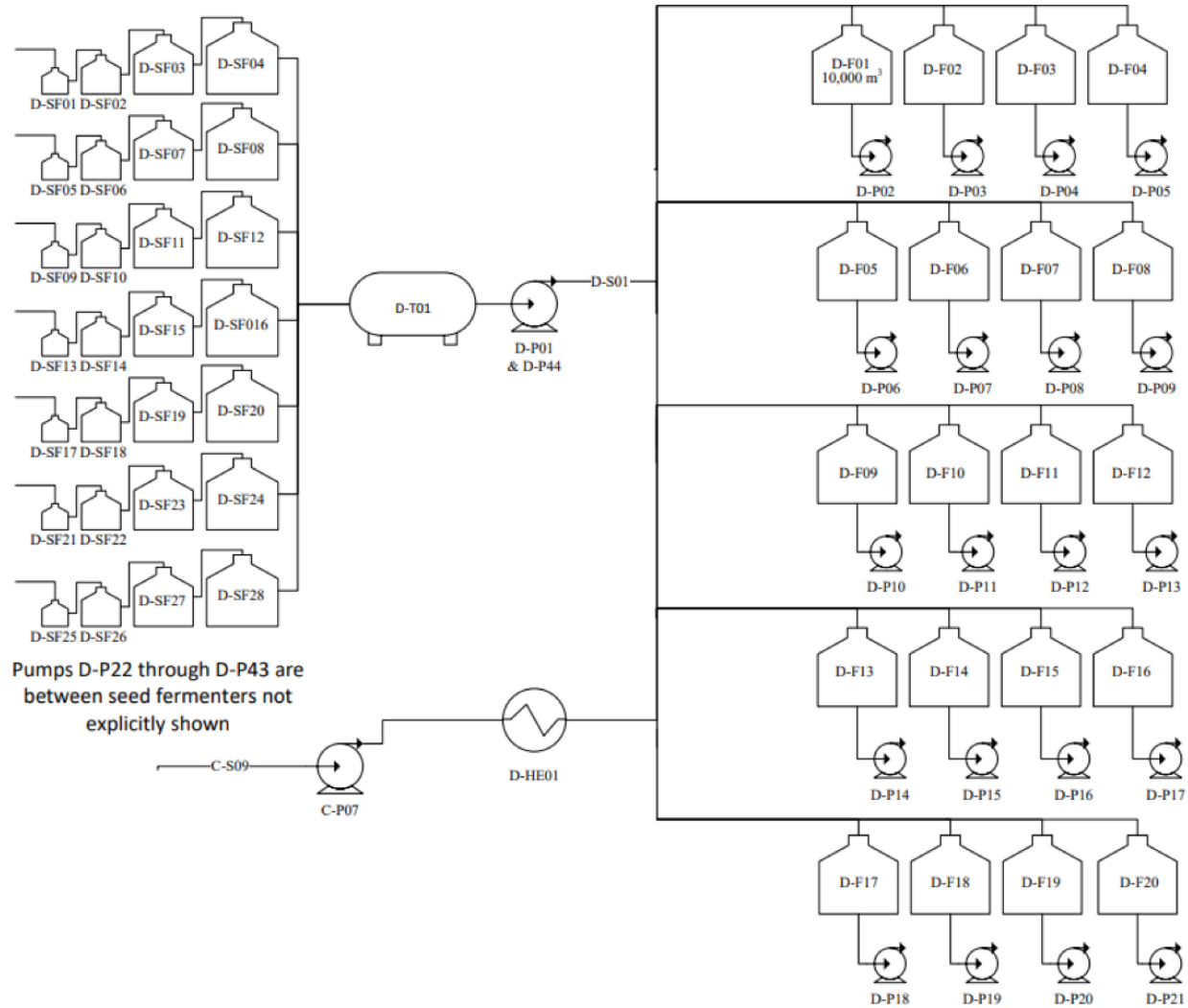


Figure 9.5a Fermentation Final Design

Table 9.5a Streams for Block D - Fermentation

Stream	D-S01	D-S02
Flow rate [kg/hr]	1200**	1,434,000
H2O [wt. %]		97.85
Glucose [wt. %]		0.13
Acetone [wt. %]		0.10
Butanol [wt. %]		0.62
Ethanol [wt. %]		0.08
Biomass [wt. %]	100.00	0.03
Metabolites & CO2 [wt. %]		1.19

**This is in kg/cycle/fermenter, not kg/hr -- this is not fed continuously

9.5.1 Seed Fermentation

To meet the *Clostridium acetobutylicum* demands of the primary fermenters, 7 groups of 4 consecutive seed fermenters with sizes 0.5 m³, 5 m³, 50 m³, and 500 m³ (D-SF01 through D-SF28) are required. Pumps D-P22 through D-P43 are used to transport cell solutions to and from each seed fermenter. The cell volume coming out of each of the 7,500 m³ seed fermenters combines into stream D-S01, which passes through pumps D-P01 and D-P44 and then is temporarily stored in surge tank D-T01. D-S01 is fed into 18 primary fermenters D-F01 through D-F18, each with a capacity of 10,000 m³. There are two additional fermenters D-F19 and D-F20 that are kept as process leeway. A small capital allowance will be designated for a working cell bank, so that the plant has the capacity to do startup fermentation.

9.5.2 Primary Fermentation

Glucose solution from the neutralization process (C-S09) passes through pump C-P11. C-S09 is then heated from the neutralization exit temperature of 31.7 °C to 37 °C, the ideal

temperature for clostridium, in heat exchanger D-HE01. C-S09 is then fed into the fermenters D-F01 through D-F18. These fermenters are continuously drained and the exiting stream passes through a pump associated with each primary fermenter. These pumps, D-P02 through D-P19, move the fermentation product into the separation block. The backup tanks D-F19 and D-F20 also have pumps D-P20 and D-P21, respectively, in the event that they need to be put into operation.

9.6 Separations (Block E)

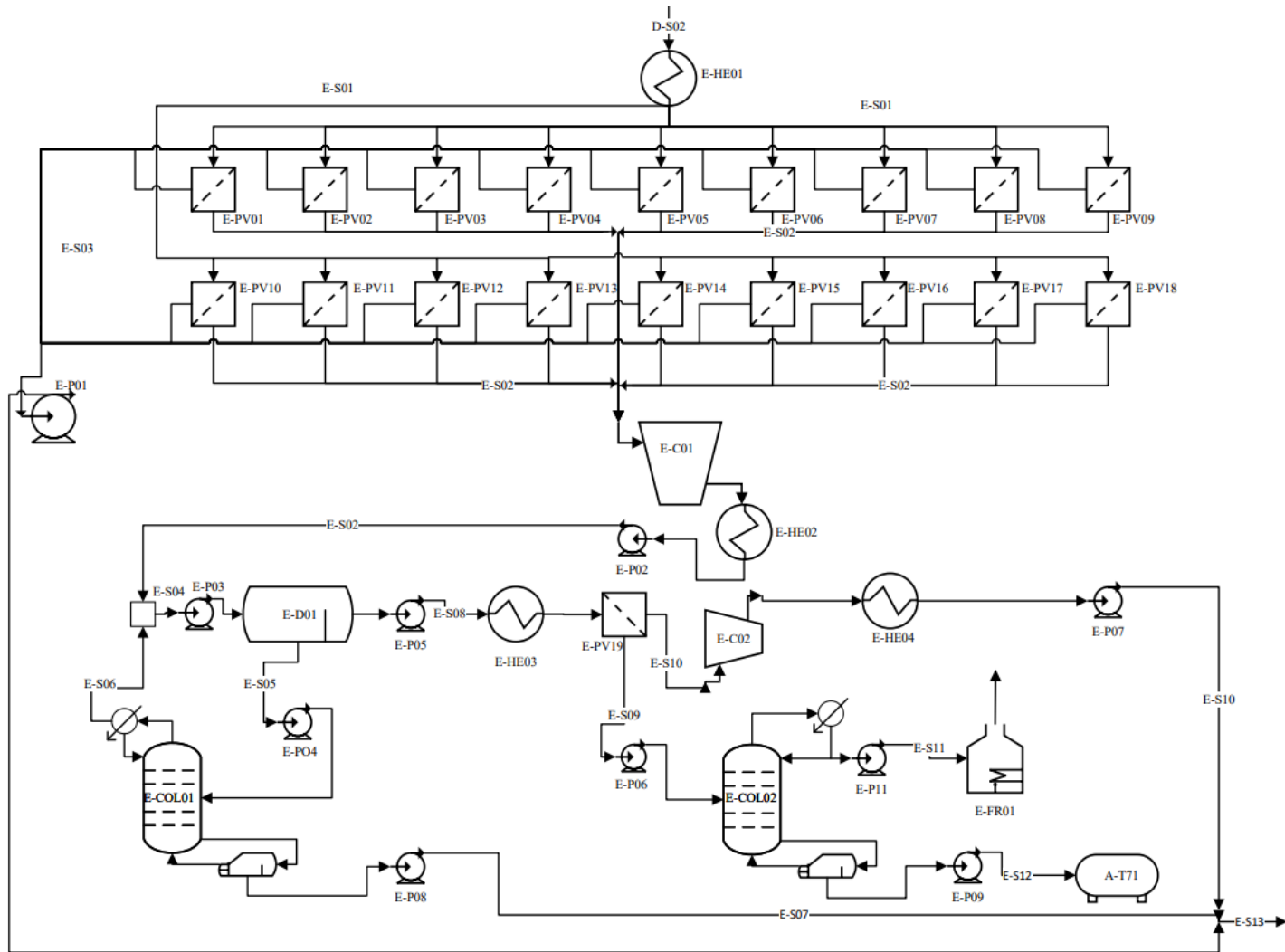


Figure 9.6a Separations Final Design

Table 9.6a Streams for Block E - Separations

Stream	E-S01	E-S02	E-S03	E-S04	E-S05	E-S06	E-S07
Flow rate [kg/hr]	1,418,000	39,000	1,379,000	65,000	48,000	29,000	22,000
H2O* [wt. %]	99.16	73	99.9	69.6	81.1	64.4	100
Acetone [wt. %]	0.10	3.6		7.1	6.4	12.4	
Butanol [wt. %]	0.63	20.5	0.07	20.9	11.6	21.5	
Ethanol [wt. %]	0.08	2.9		2.4	0.9	1.7	
Biomass [wt. %]	0.03		0.03				

*tr. metabolites and glucose stay with water

Table 9.6a (continued)

Stream	E-S08	E-S09	E-S10	E-S11	E-S12	E-S13
Flow rate [kg/hr]	17,000	10,000	7,000	2,000	7,000	1,386,000
H2O [wt. %]	38		88.1	0.4	0.1	99.84
Acetone [wt. %]	8	11	4.0	44.7		0.02
Butanol [wt. %]	47	77	7.5	6.2	99.9	0.11
Ethanol [wt. %]	7	12	0.4	48.7		
Biomass [wt. %]						0.03

*tr. metabolites and glucose stay with water

Residual cell matter, ABE products, and water pass through stream E-S01 and into heat exchanger E-HE01 where the temperature is heated from 37 °C to 60°C. E-S01 then splits between 18 hydrophobic pervaporation filters (E-PV01 through E-PV18) each with an area of 212 m³. These POMS filters were designated as hollow fiber membranes that typically have poor fouling resistance but are relatively cheap. To mitigate membrane fouling, the area of each membrane was increased to 281 m³. The retentate from each unit, which contains the cell matter and majority water, combines into stream E-S03 and is passed through pump E-P01 towards acid pretreatment for recycling. The filtrate of E-PV01 through E-PV18 combines into stream E-S02 which passes through compressor E-C01 that generates a pressure from 280 Pa to 0.707 atm.

E-S02 then passes through condenser E-HE02 which adjusts the temperature from 105 to 25°C. Pump E-P02 facilitates the movement of stream E-S02 along to the decanter process with the corresponding recycle column..

E-S02, which contains the ABE products and water, then combines with stream E-S06, which is the water/ABE azeotrope mixture that has come out of the decanter recycle column E-COL01. These combined streams make stream E-S04 which passes through pump E-P03 that pushes the water and ABE products into decanter E-D01, which is a 13.5 m³ volume decanter that separates the stream into aqueous and organic layers. In order to increase butanol yield, the aqueous layer is sent to the decanter recycle column E-COL01 as the feed in stream E-S05 via pump E-P04. The tops product of E-COL01 is the previously mentioned stream E-S06. The bottoms product of E-COL01, stream E-S07, is a water stream and acts as a means to purge the system of water to make the main decanting process (E-D01) more effective while ensuring butanol is not lost. Whereas the aqueous phase E-S05 was recycled, the organic phase of E-D01 leaves the decanter in stream E-S08 and passes through pump E-P05 and heat exchanger E-HE03, which changes the temperature of E-S08 from 25 °C to 60 °C. Stream E-S08 then enters the hydrophilic pervaporation filter E-PV19, which is classified as a ceramic PDMS type of membrane, with a total area of 11,000 m².

The permeate of E-PV19, stream E-S10, contains primarily water and is sent through compressor E-C02 which changes the pressure from 280 Pa to 0.707 atm. E-S10 then passes through condenser E-HE04 (to adjust from 60°C to 25°C) and then travels through pump E-P07, which raises the pressure to 1 atm. E-S10 then combines with stream E-S03 from E-PV01 through E-PV18 and E-S07 from column E-COL01 to form the water recycle stream E-S13. The retentate of E-PV19 is stream E-S09, which contains ABE products and trace water. E-S09 is

sent to the ABE distillation column E-COL02, which separates the butanol from the acetone and ethanol. Acetone and ethanol come out of the top of E-COL02 in stream E-S11 which is sent to furnace E-FR01 where they are burned to supplement energy use in the plant. The bottoms product of E-COL02 is final butanol product that is sent in stream E-S12 to product storage tank A-T71 where it is stored until it is shipped to the customer.

10. Conclusions and Recommendations

The above presented design is the team's final recommended process. However, the team would like to conclude with possible future research suggestions, design improvements, and future extensions of the capstone itself.

10.1 Future Research Suggestions

The novel nature of this process means that there are several parts of the design that could benefit from additional research. The following sections highlight the areas that the team feels need to be more thoroughly understood so that the best design and an accurate economic analysis can be put forth.

10.1.1 CaHPO₄ Animal Feed

The post-hydrolysis corn waste was combined with the neutralization salt calcium monohydrogen phosphate to create what the team has determined to be a potential nutritional animal feed supplement. As of right now there is not substantial evidence to support this use of the waste stream. Additional research needs to be done to show that this product can be digested by cows and has nutritional benefits so it can be marketed appropriately. More research must be done into the economic value of this product. This is the highest revenue product from this plant, thus it is imperative that the correct value can be assigned to the animal feed based on the

calcium monohydrogen phosphate and corn content. This will give a better understanding of the economic viability of the plant as a whole.

10.1.2 Clostridium

One potential area for research would be the ABE fermentation bacteria. Looking into alternative strains of bacteria, or at the very least better understanding the kinetics of the clostridium currently used in this project, could help the team make the fermentation process more efficient. In researching for this project, the team identified a number of research papers detailing genetically engineered Clostridium bacteria capable of increased butanol survivability and production rate. However, these novel strains do not have well-studied kinetic data with which to build a model so a more traditional strain, ATCC 824, was used.

10.1.3 Simulation environments

During the completion of this process design, an inability to model necessary processes in a computational simulation environment arose for cellulose hydrolysis, pervaporation, and decantation. While glucose was part of the software, Aspen lacked the available components for accurate modeling of cellulose polymer hydrolysis. Pervaporation was missing from Aspen as an available unit operation. Similarly, challenges were encountered when decantation was attempted in MATLAB for the two-phase, four component decantation of the ABE and water product stream. No other modeling environments could be located for these three cases, thus more manual workarounds in MATLAB and by-hand calculations were used.

Future research should be done to either develop or locate more effective simulation models for cellulose hydrolysis, pervaporation, and complex decantation.

10.2 Design Improvements

The team also would like to acknowledge the design aspects of this project that could have been improved or optimized given a longer timeline or more extensive research. The scope of this project was rather large—it included biological processes, advanced separation techniques, and many novel, non-commercialized design processes. The following sections detail some specific parts of the complex design that the team wished they could have improved upon.

10.2.1 Evaluating Solids Removal

Post-Neutralization, nearly the entirety of our animal feed supplement is removed via a disk filter. While there is data to support this, it does not account for the potential formation of a cake layer and rapid fouling. If the process were to be developed further, an analysis of the possibility of these occurring should be conducted. Furthermore, it may be worthwhile to replace this filter with a continuous centrifuge such that fouling is no longer a concern and possibly reducing the water volume ejected in our product.

10.2.2 Optimizing Fermentation Parameters

The bulk of the team's continuous fermentation design was based on work by Buehler and Mesbah: "Kinetic Study of Acetone-Butanol-Ethanol Fermentation in Continuous Culture". MATLAB code was written to reflect the mass balances, rate equations, and kinetic parameters used in the paper, except with our input glucose and biomass concentrations. The only way the team could prevent washout and get the model to converge with the new inputs was to make the dilution rate very small: 0.01/hr. This value established the volume sizing of the fermentation tanks at a very large 10,000 m³. This volume is extremely large in comparison to standard, commercially available fermentation tanks of today. This suggests that this dilution rate, or other

fermentation parameters, could have been better optimized to potentially lower the large equipment capital costs associated with these fermentation tanks.

10.2.3 Separations: Decantation

Another large target for improvement is within the team's separation processes. The team was excited by the idea of using a separation technique based on selective vacuum filtering as opposed to relying on mastering the thermodynamics of the ABE-water azeotrope in distillation. This azeotrope was eventually addressed between pervaporation steps in the decantation step and recycle column. The team was able to achieve two-phase separation, but it was on the edge of the envelope. To ensure a more reliable and stable decantation step, it would be more ideal if this feed composition sat more thoroughly in the two-phase region. This could have been ensured with another separation step added after hydrophobic pervaporation to pull out more water before decantation, or through a more optimized recycle column post decantation that pulls out even more water than it already does.

10.2.4 Pumps

The current plant design has pumps where necessitated by process demands with a spare design for each pump. It has been determined that having a "back-up" pump for each existing pump is not economically prudent. A better design would possibly be a single back-up pump designed for each group of repeating pumps. A future design improvement would be addressing this back-up pump redundancy to make the plant more economically efficient.

10.2.5 Pervaporation

Improvements in pervaporation processes should consider 1) the possible variability of membrane operating pressures, 2) the effects of fouling and other contamination methods associated with the coupling of an ABE fermentation and pervaporation membranes and 3) new

materials that can offer increased selectivity with respect to solvent extraction. Pervaporation is largely absent from contemporary industrial fermentation processes for these reasons, as well as a reliance on other separation techniques. Pervaporation technologies therefore have not seen much implementation outside of the lab scale, although those results are very promising. Optimization should be coupled with new research in order to cut down on the capital and operating costs associated with pervaporation, or by implementing different pervaporation configurations to improve water removal and/or solvent uptake.

10.2.6 Waste Disposal

The waste disposal considerations of this design were mostly mitigated by the reliance on recycling within the process and the ability to turn much of our waste into marketable commodities. Thus, the actual waste generated through this process is limited to the carbon dioxide generated in fermentation, and the waste biomass accumulated during fermentation. Both of these waste products are generated in minimal quantities relative to the other process products. As such, the associated costs have been folded into other equipment operation costs and not independently evaluated. Future work can optimize the waste management aspect by investigating the possibility of recycling or incinerating biomass on site or the implementation of carbon-capture techniques to be used in conjunction with the fermenters.

10.3 Future Extensions of the Project / Continued Work

If another capstone group were to continue the work completed here, there are several areas that the team recommends expanding upon:

- Looking into pressure swing distillation / traditional methods of ABE separation to compare energy and capital costs with pervaporation

- Researching other possible hydrolysis processes for better yield or economic outcomes: alkaline, dilute sulfuric acid
- Batch fermentation to compare with continuous fermentation currently in use
- Looking at ways to mitigate milling loss, possibly via the examination of alternative milling process types
- Looking into possible alternative acid pretreatment waste product markets, such as fertilizer or other agricultural supplements
- Determining the economic factors that can be affected by considering what subsidies and other financial incentives are offered to biofuel producers

10.4 Final Recommendations

Given all of the information presented in this report, the decision of whether to go forward with this design hinges on the economic viability of the plant. With an IRR of 13.9%, this investment does represent a potentially profitable endeavor, however, the uncertainty surrounding our key revenue driver, the animal feed product, affects the reliability of any economic predictions. The product-market fit and pricing of the animal feed must be verified before prospective investors can feel confident in this butanol plant. Additionally, there are other technical risks associated with this project that call into question its prudence as an investment. The fermentation modeling, for example, should be verified given that it is highly sensitive to glucose concentration from acid pretreatment. The use of corn stover as a feedstock for large-scale fermentation and pervaporation filters to separate ABE products are both novel for this industry and thus need to be proven before investment. The stability of the agricultural field also heavily affects the project at hand given the dependence on buying farming waste and the sale of the animal feed back into the farming sector.

With all of this in mind, the team does not recommend this design as it currently exists. This is not a definitive rejection of the design, but rather a comment on the inherent risk of an investment with key products entering an uncertain market. With the technical and economic approach taken, the team posits that there is too much uncertainty to venture a financial stake of this magnitude.

11. Acknowledgements

We would like to extend our sincere appreciation to the esteemed individuals within the Chemical Engineering Department at the University of Virginia, whose invaluable contributions were instrumental in the successful completion of this project.

First and foremost, we would like to thank Professor Eric Anderson for providing oversight and direction throughout this design. We would also like to thank Professor Ron Unnerstall for providing insights into process safety as well as industrial processes as a whole. Furthermore, we are grateful for the biotechnical insights provided by Professor George Prpich, which significantly enhanced the depth and quality of our project outcomes.

Lastly, we would like to extend our appreciation to all of the Chemical Engineering professors who have taught us over the years. Without their dedication to our education and their unwavering support, we would not have completed this capstone, nor would we be where we are today.

12. References

A refresher on Net present value. Harvard Business Review. (2017, December 6).

<https://hbr.org/2014/11/a-refresher-on-net-present-value>

Alternative Fuels Data Center. (2019). Alternative Fuels Data Center: Biobutanol. Energy.gov.

https://afdc.energy.gov/fuels/emerging_biobutanol.html

Avci, A., Saha, B. C., Kennedy, G. J., & Cotta, M. A. (2013). High temperature dilute phosphoric acid pretreatment of corn stover for furfural and ethanol production. *Industrial Crops and Products*, 50, 478–484. <https://doi.org/10.1016/j.indcrop.2013.07.055>

Aspen Technology. (1999). *Modeling Processes with Electrolytes*. Aspen Technology.

<https://sites.chemengr.ucsb.edu/~ceweb/courses/che184b/aspenplus/GettingStartedElectrolytes.pdf>

Baral, N. R., Slutzky, L., Shah, A., Ezeji, T. C., Cornish, K., & Christy, A. (2016).

Acetone-butanol-ethanol fermentation of corn stover: Current production methods, economic viability and commercial use. *FEMS Microbiology Letters*, 363(6).

<https://doi.org/10.1093/femsle/fnw033>

Berry, C., McNeely, A., Beauregard, K., & Geddie, J. E. (2012). N.C. Department of Labor Occupational Safety and Health Program.

Board of governors of the Federal Reserve System. Federal Reserve Board - H.15 - Selected Interest Rates (Daily) - March 29, 2024. (2024, March).

<https://www.federalreserve.gov/releases/h15/>

Buehler, E. A., & Mesbah, A. (2016). Kinetic Study of Acetone-Butanol-Ethanol Fermentation in Continuous Culture. *PLOS ONE*, 11(8), e0158243.

<https://doi.org/10.1371/journal.pone.0158243>

Buendia-Kandia, F., Rondags, E., Framboisier, X., Mauviel, G., Dufour, A., & Guedon, E.

(2018). Diauxic growth of *Clostridium acetobutylicum* ATCC 824 when grown on mixtures of glucose and cellobiose. *AMB Express*, 8, 85. <https://doi.org/10.1186/s13568-018-0615-2>

Calcium hydroxide - nj.gov. (n.d.).

<https://www.nj.gov/health/eoh/rtkweb/documents/fs/0322.pdf>

Calcium hydroxide supply chain - full profile. (n.d.-a).

[https://www.epa.gov/system/files/documents/2023-03/Calcium Hydroxide Supply Chain Profile.pdf](https://www.epa.gov/system/files/documents/2023-03/Calcium%20Hydroxide%20Supply%20Chain%20Profile.pdf)

Chemical Engineering Plant Cost Index. Fluid mechanics. (2023).

<https://www.training.itservices.manchester.ac.uk/public/gced/CEPCI.html?reactors%2FCEPCI%2Findex.html>

Clifford, C. (2023). *Alternative Fuels From Biomass Sources*. 10.3 Economics of Butanol

Production | EGEE 439: Alternative Fuels from Biomass Sources.

<https://www.e-education.psu.edu/egee439/node/721>

Cook, R. (2023, November 4). *Ranking of states that produce the most corn*. Beef2Live.

<https://beef2live.com/story-states-produce-corn-0-107129#:~:text=The%20Most%20Corn,Iowa%20produced%20the%20most%20corn%20in%20the%20United%20States%20in,Illinois%2C%20Nebraska%2C%20%26%20Minnesota.>

Cooling water cost: Industrial utilities. Cooling Water Costs | Current and Forecast | Intratec.us.

<https://www.intratec.us/products/water-utility-costs/commodity/cooling-water-cost>

DCCEEW. (2022). *Phosphoric acid - DCCEEW*. Dcceew.gov.au; Department of Climate

Change, Environment, Energy and Water of Australia.

<https://www.dcceew.gov.au/environment/protection/npi/substances/fact-sheets/phosphoric>

<https://www.osti.gov/servlets/purl/1392775>

Ibrahim, N. H., Ibrahim, W. H. W., & Sakinah, A. M. M. (2017). Simulation of Dilute Acid hydrolysis of Wood Sawdust for Xylose Production using Aspen Plus.

PIET-18, PABEMS-18, MEHSS-18 & LBEIS-18 Sept. 17-19, 2018 Paris (France). Sept. 17-19, 2018 Paris (France). <https://doi.org/10.17758/EIRAI4.F0918232>

Industrial Steam Cost: Industrial Utilities. Industrial Steam Cost | Current and Forecast | Intratec.us. (n.d.).

<https://www.intratec.us/products/water-utility-costs/commodity/industrial-steam-cost>

Iowa Admin. Code r. 567-149.4 - Fee schedule. (n.d.). LII / Legal Information Institute; Cornell University. Retrieved March 31, 2024, from

<https://www.law.cornell.edu/regulations/iowa/Iowa-Admin-Code-r-567-149-4>

Iowa Corn Growers Association (2024). Corn FAQs.

<https://www.iowacorn.org/education/faqs#:~:text=In%20Iowa%2C%20some%20farmers%20begin,isn%27t%20harvested%20until%20November.>

Iowa Legislature. (2008, July 2). IAC 7/2/08 environmental protection[567] ch 109, p.1 ... Iowa Legislature. <https://www.legis.iowa.gov/docs/iac/chapter/567.109.pdf>

Jiao, H. (2016, June 2). *To harvest stover or not: Is it worth it?*. farmdoc daily.

<https://farmdocdaily.illinois.edu/2016/02/to-harvest-stover-or-not-is-it-worth-it.html>

Knozowska, K., Kujawska, A., Li, G., Kujawa, J., Bryjak, M., Kujawski, W., Lipnizki, F., Ahrné, L., Petrinić, I., & Kujawski, J. K. (2021). Membrane assisted processing of acetone, butanol, and ethanol (ABE) aqueous streams. *Chemical Engineering and Processing - Process Intensification*, 166, 108462. <https://doi.org/10.1016/j.cep.2021.108462>

Kujawska, A., Knozowska, K., Kujawa, J., & Kujawski, W. (2016). Influence of downstream

- pressure on pervaporation properties of PDMS and POMS based membranes. *Separation and Purification Technology*, 159, 68–80. <https://doi.org/10.1016/j.seppur.2015.12.057>
- Liu, G., Wei, W., & Jin, W. (2013). Pervaporation Membranes for Biobutanol Production. *ACS Sustainable Chemistry & Engineering*, 2(4), 546–560. <https://doi.org/10.1021/sc400372d>
- Liu, G., Wei, W., Wu, H., Dong, X., Jiang, M., & Jin, W. (2011). Pervaporation performance of PDMS/ceramic composite membrane in acetone butanol ethanol (ABE) fermentation–PV coupled process. *Journal of Membrane Science*, 373(1-2), 121–129. <https://doi.org/10.1016/j.memsci.2011.02.042>
- Liu, X.-B., Gu, Q.-Y., Yu, X.-B., & Luo, W. (2012). Enhancement of butanol tolerance and butanol yield in *Clostridium acetobutylicum* mutant NT642 obtained by nitrogen ion beam implantation. *Journal of Microbiology (Seoul, Korea)*, 50(6), 1024–1028. <https://doi.org/10.1007/s12275-012-2289-9>
- Macdonald, D. G., Bakhshi, N. N., Mathews, J. F., Roychowdhury, A., Bajpai, P., & Moo-Young, M. (1983). Alkali treatment of corn stover to improve sugar production by enzymatic hydrolysis. *Biotechnology and bioengineering*, 25(8), 2067–2076. <https://doi.org/10.1002/bit.260250815>
- Mani, S., Tabil, L. G., & Sokhansanj, S. (2004). Grinding performance and physical properties of wheat and barley straws, corn stover and switchgrass. *Biomass and Bioenergy*, 27(4), 339–352. <https://doi.org/10.1016/j.biombioe.2004.03.007>
- Million Bushel Bins*. Sukup. (n.d.). <https://www.sukup.com/products/million-bushel-bin>
- Moon, H. G., Jang, Y.-S., Cho, C., Lee, J., Binkley, R., & Lee, S. Y. (2016). One hundred years of clostridial butanol fermentation. *FEMS Microbiology Letters*, Vol. 363. <https://doi.org/10.1093/femsle/fnw001>

NASA (2023, March 23). Planes, Shipping Lanes, and Automobiles. NASA Global Climate Change. <https://climate.nasa.gov/news/3258/planes-shipping-lanes-and-automobiles/#:~:text=That%20changed%20once%20we%20began%20burning%20fossil%20fuels,emissions%2C%20second%20only%20to%20the%20electric%20power%20sector.>

Niemistö, J., Kujawski, W., & Keiski, R. L. (2013). Pervaporation performance of composite poly(dimethyl siloxane) membrane for butanol recovery from model solutions. *Journal of Membrane Science*, 434, 55–64. <https://doi.org/10.1016/j.memsci.2013.01.047>

Peters, M., Timmerhaus, K., & West, R. (2003). *Plant Design and Economics for Chemical Engineers* (Fifth). The McGraw-Hill Companies.

Phosphoric acid 75%. (n.d.-b). https://www.chemcentral.com/media/product_attribute/sds_file/s/d/sds_file-16142350.pdf

Process water cost: Industrial Utilities. Process Water Costs | Current and Forecast | Intratec.us. (n.d.). <https://www.intratec.us/products/water-utility-costs/commodity/process-water-cost>

Pudjiastuti, L., Widjaja, T., Iskandar, K. K., Sahid, F., Nurkhamidah, S., Altway, A., & Putra, A. P. (2021). Modelling and simulation of multicomponent acetone-butanol-ethanol distillation process in a sieve tray column. *Heliyon*, 7(4), e06641. <https://doi.org/10.1016/j.heliyon.2021.e06641>

Pump Power Calculator. *Engineering ToolBox*. (2023, November 7). https://www.engineeringtoolbox.com/pumps-power-d_505.html

Purified phosphoric acid. (n.d.-d). <https://isolab.ess.washington.edu/resources/H3PO4.pdf>

Rao, A., Sathiavelu, A., & Mythili, S. (2016). Genetic Engineering In BioButanol Production And Tolerance. *Brazilian Archives of Biology and Technology*, 59, e16150612. <https://doi.org/10.1590/1678-4324-2016150612>

Safety Data Sheet: Phosphoric Acid. (n.d.-e).

https://beta-static.fishersci.com/content/dam/fishersci/en_US/documents/programs/education/regulatory-documents/sds/chemicals/chemicals-o/S25470B.pdf

Schweitzer, P. A. (1979). *Handbook of separation techniques for chemical engineers*. McGraw Hill.

State corporate income tax rates and brackets for 2024. Tax Foundation. (2024, February 5).

<https://taxfoundation.org/data/all/state/state-corporate-income-tax-rates-brackets-2024/>

Stewart, M. (2008, January 1). *Chapter 4 - Three-Phase Oil and Water Separators* (M. Stewart & K. Arnold, Eds.). ScienceDirect; Gulf Professional Publishing.

<https://www.sciencedirect.com/science/article/pii/B9780750689793000040>

Strauch, B., & Stockton, M. (2013, September). *Feed Cost Cow-Q-Lator*. University of Nebraska - Lincoln; UNIL.

<https://extensionpubs.unl.edu/publication/g2214/pdf/view/g2214-2013.pdf>

Tenenbaum D. J. (2008). Food vs. fuel: diversion of crops could cause more hunger.

Environmental health perspectives, 116(6), A254–A257.

<https://doi.org/10.1289/ehp.116-a254>

Thessen, G., Maliszewski, S., & Dahlman, A. (2023, October). *2023 Iowa Agricultural Statistics*.

USDA National Agricultural Statistics Service; U.S. Department of Agriculture.

https://www.nass.usda.gov/Statistics_by_State/Iowa/Publications/Annual_Statistical_Bulletin/2023-Iowa-Annual-Bulletin.pdf

Trindade, W. R., & Santos, R. G. (2017). Review on the characteristics of butanol, its production and use as fuel in internal combustion engines. *Renewable and Sustainable Energy Reviews*,

69, 642–651. <https://doi.org/10.1016/j.rser.2016.11.213>

Um, B. H., Karim, M., & Henk, L. (2003). Effect of sulfuric and phosphoric acid pretreatments on enzymatic hydrolysis of corn stover. *Applied biochemistry and biotechnology*, 105 -108, 115–125. <https://doi.org/10.1385/abab:105:1-3:115>

United Nations (2023). *Causes and Effects of Climate Change*. United Nations Climate Action. <https://www.un.org/en/climatechange/science/causes-effects-climate-change>

U.S. Bureau of Labor Statistics. (2023, April 25). Chemical plant and System Operators. U.S. Bureau of Labor Statistics. <https://www.bls.gov/Oes/current/oes518091.htm>

USDA (2023, September 28). *Feed Grains Sector at a Glance*. USDA - Economic Research Service. <https://www.ers.usda.gov/topics/crops/corn-and-other-feed-grains/feed-grains-sector-at-a-glance/>

US Department of Commerce, N. (n.d.). National Weather Service. <https://www.weather.gov/>

Wang, Q., Wei, W., Li, X., Sun, J., He, J., and He, M. (2016). Comparative study of alkali and acidic cellulose solvent pretreatment of corn stover for fermentable sugar production. *BioRes.* 11(1), 482-491.

Watson, G. (2023, July 25). *Combined state and federal corporate income tax rates in 2022*. Tax Foundation. [URL](#)

Wu, S., (2009, June 8). *Reciprocating pumps vs. multi-stage centrifugal pumps*. Pumps and Systems Magazine. [https://www.pumpsandsystems.com/reciprocating-pumps-vs-multi-stage-centrifugal-pumps#:~:text=The%20overall%20efficiency%20of%20a,range%20\(see%20Figure%204\)](https://www.pumpsandsystems.com/reciprocating-pumps-vs-multi-stage-centrifugal-pumps#:~:text=The%20overall%20efficiency%20of%20a,range%20(see%20Figure%204))

Wilson, J. (2011). A COST ANALYSIS FOR THE DENSIFICATION AND TRANSPORTATION OF CELLULOSIC BIOMASS FOR ETHANOL PRODUCTION. <https://krex.k-state.edu/>

Zhou, H., Su, Y., & Wan, Y. (2014). Phase separation of an acetone–butanol–ethanol (ABE)–water mixture in the permeate during pervaporation of a dilute ABE solution.

Separation and Purification Technology, 132, 354–361.

<https://doi.org/10.1016/j.seppur.2014.05.051>